Ore Geology Reviews 48 (2012) 460–473

Contents lists available at SciVerse ScienceDirect

Ore Geology Reviews

journal homepage: www.elsevier.com/locate/oregeorev

Relationships between porphyry Cu–Mo mineralization in the Jinshajiang–Red River metallogenic belt and tectonic activity: Constraints from zircon U–Pb and molybdenite Re–Os geochronology

Leiluo Xu [a,b], Xianwu Bi [a,*], Ruizhong Hu [a], Xingchun Zhang [a], Wenchao Su [a], Wenjun Qu [c], Zhaochu Hu [d], Yongyong Tang [a,b]

[a] State Key Laboratory of Ore Deposit Geochemistry, Institute of Geochemistry, Chinese Academy of Sciences, Guiyang, 550002, China
[b] Graduate University of Chinese Academy of Sciences, Beijing, 100049, China
[c] National Research Center of Geoanalysis, Chinese Academy of Geological Sciences, Beijing, 100037, China
[d] State Key Laboratory of Geological Processes and Mineral Resources, China University of Geosciences, Wuhan, 430074, China

ARTICLE INFO

Article history:
Received 8 December 2011
Received in revised form 9 May 2012
Accepted 9 May 2012
Available online 30 June 2012

Keywords:
Jinshajiang–Red River Porphyry Cu–Mo metallogenic belt
Porphyry Cu–Mo deposit
Tectonic activity
Zircon U–Pb age
Molybdenite Re–Os age

ABSTRACT

The Jinshajiang–Red River porphyry Cu–Mo metallogenic belt is an important Cenozoic porphyry Cu–Mo mineralization concentrating zone in the eastern Indo-Asian collision zone. New zircon U–Pb and molybdenite Re–Os ages and compilation of previously published ages indicate that porphyry Cu–Mo deposits in the belt did not form at the same time, i.e., the porphyry emplacement and relevant Cu–Mo mineralization ages of the Ailaoshan–Red River ore belt in south range from 36.3 Ma to 34.6 Ma, and from 36.0 Ma to 33.9 Ma, respectively, which are obviously younger than the porphyry emplacement ages of 43.8–36.9 Ma and the relevant Cu–Mo mineralization ages of 41.6–35.8 Ma of the Yulong ore belt in north. Tectonic studies indicated that the Jinshajiang fault system in north and Ailaoshan–Red River fault system in south of the Jinsjiang–Red river belt had different strike-slip patterns and ages. The right-lateral strike-slip motion of the Jinshajiang fault system initiated at ca. 43 Ma with corresponding formation of the Yulong porphyry Cu–Mo system, whereas the left-lateral strike-slip motion of the Ailaoshan–Red River fault system initiated at ca. 36 Ma with corresponding formation of the Ailaoshan–Red River porphyry Cu–Mo system. Therefore, the different ages of porphyry Cu–Mo systems, between in north and south of the Jinshajiang–Red River belt, indicate that the porphyry Cu–Mo mineralization is closely related to the divergent strike-slip movements between the Jinshajiang and Ailaoshan–Red River strike-slip faulting resulted from the Indo-Asian collision. The tanslithospheric Jinshajiang–Red River faulting caused partial melting of the enriched mantle sources of alkali-rich porphyries by depressurization or/and asthenospheric heating, and facilitated the migration of alkali-rich magmas and the corresponding formation of alkali-rich porphyries and relevant Cu–Mo deposits in the belt.

1. Introduction

The Jinshajiang–Red River porphyry Cu–Mo metallogenic belt, extending for more than 1500 km, is an important belt with abundant Cu–Mo mineralization in the eastern Indian–Asian collision zone. This porphyry Cu–Mo metallogenic belt is important for the understanding of porphyry Cu–Mo deposits in an intra-continental setting, and has been a subject of numerous previous studies (Bi, 1999; Bi et al., 1999, 2002, 2004, 2005, 2006, 2009; Hou et al., 2003, 2005, 2006, 2007a,b,c; Liang, 2002; Liang et al., 2002, 2004, 2006a,b, 2007, 2008, 2009a,b).

Porphyries and related Cu–Mo deposits in the Jinshajiang–Red River belt are primarily controlled by the Jinshajiang–Red River strike-slip fault, which resulted from the Indo-Asian collision (Fig. 1; Hou et al., 2006, 2007a). Over the past decades, studies addressing relationships between porphyries and Cu–Mo deposits, including porphyry emplacement and mineralization ages, occurrences of porphyries and ore-bodies, originations of ore-forming materials, all indicated that the porphyry Cu–Mo deposits of the belt were genetically associated with the Cenozoic Jinshajiang–Red River alkali-rich porphyries (Bi, 1999; Bi et al., 1999, 2002, 2004, 2009; Gu et al., 2003; Hou et al., 2006, 2007a,b; Hu et al., 1998, 2004; Wang et al., 2004; Xu et al., 2007, 2011). At the meantime, isotopic age data using major K–Ar, Rb–Sr and Sm–Nd methods and minor Ar–Ar, U–Pb and Re–Os methods for both alkali-rich porphyries and related Cu–Mo deposits have been rapidly accumulated in the literature (Deng et al., 1998; Hou et al., 2003, 2006; Wang et al., 2004; Xie et al., 1984; Zeng et al., 2002; Zhang and Xie, 1997; Zhang et al., 1987). These age data indicate that alkali-rich porphyries and related Cu–Mo deposits were mainly formed at 40–30 Ma, and there is no remarkable age difference from south to north along the Jinshajiang–Red River

* Corresponding author. Tel.: +86 851 5891962; fax: +86 851 5891664.
E-mail address: bixianwu@vip.gyig.ac.cn (X. Bi).

0169-1368/$ – see front matter © 2012 Elsevier B.V. All rights reserved.
doi:10.1016/j.oregeorev.2012.05.010

belt. The porphyries and related Cu–Mo deposits were considered to be formed at the same time and in the same geodynamic environment (Wang et al., 2004; Xie et al., 1984; Zhang et al., 1987).

Accompanying the rapid progress in high-precision dating methods over the past decade, a number of significant zircon U–Pb and molybdenite Re–Os ages for alkali-rich porphyries and associated Cu–Mo deposits have been obtained (Guo et al., 2006; Hou et al., 2006; Liang et al., 2002, 2004, 2006a,b, 2008, 2009b; Wang et al., 2004). These studies mainly dealt with the ages of individual porphyry Cu–Mo deposits in the Jinshajiang–Red River belt and systematic studies on the geochronological characteristics of the whole-belt and their relation to tectonic evolution were scarce.

Recent molybdenite Re–Os dating of the Machangqing deposit, in southern segment of the belt, yielded ages of 33.9 Ma (Wang et al., 2004), 35.8 Ma (Hou et al., 2006), 35.3 Ma (Xing et al., 2009) and 34.7 Ma (He et al., 2011), which are obviously younger than ages of 40.1 Ma (Hou et al., 2006) and 41.6 Ma (Tang et al., 2009) for the Yulong deposit in northern segment of the belt. Furthermore, there are some remarkable differences in source characteristics, mineralization scales and metal grades of porphyry Cu–Mo deposits between southern and northern segments of the belt (Hou et al., 2006, 2007c; Hu et al., 2004; Xu et al., 2011). These suggest that the ore-forming ages and relevant geodynamic settings of porphyry Cu–Mo deposits may be different between southern and northern segments of the belt.

In the present study, zircon U–Pb and molybdenite Re–Os age determinations of several representative porphyry Cu–Mo deposits from the Jinshajiang–Red River belt were carried out to augment the published data. Based on the new and previous zircon U–Pb and molybdenite Re–Os ages, this paper addresses the geochronological characteristics of porphyry Cu–Mo deposits in the belt in the context

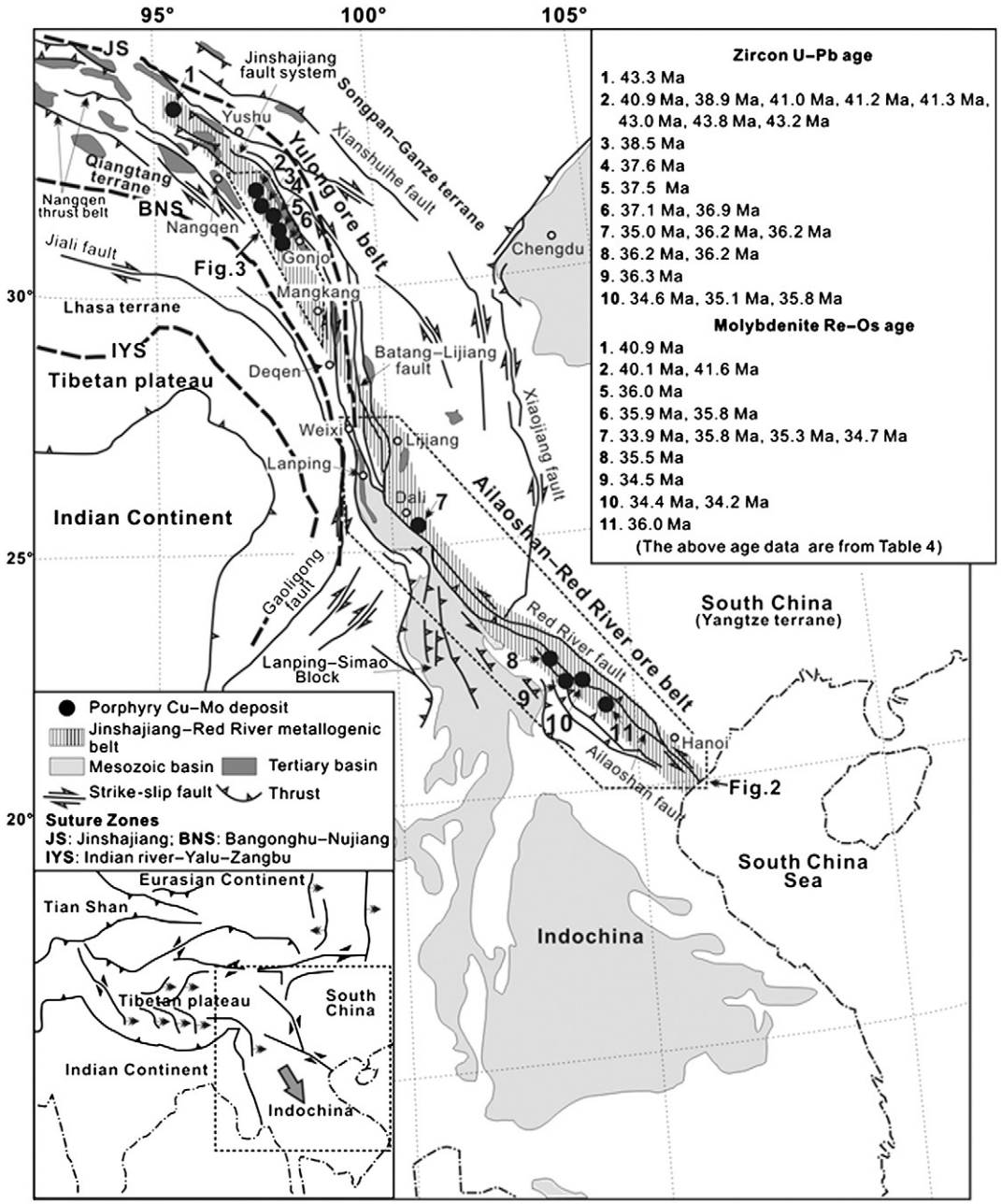

Fig. 1. Simplified geological map showing the Cenozoic tectonic framework and the distribution of porphyry Cu–Mo deposits in the Jinshajiang–Red River porphyry Cu–Mo metallogenic belt (modified from Wang et al., 2001); Porphyry Cu–Mo deposit: 1-Narigongma, 2-Yulong, 3-Zhanaga, 4-Mangzong, 5-Duoxiasongduo, 6-Malasongduo, 7-Machangqing, 8-Habo, 9-Chang'anchong, 10-Tongchang, 11-O Quy Ho.

of regional tectonic evolution. We aim to provide an insight into the ore-forming geodynamic settings of the porphyry Cu–Mo deposits in the Jinshajiang–Red River porphyry Cu–Mo metallogenic belt.

2. Geological setting

The Jinshajiang–Red River porphyry Cu–Mo metallogenic belt is adjacent to the NNW–NW-trending Jinshajiang–Red River deep fault zone in the eastern Indo-Asian collision zone. The eastern Indo-Asian collision zone comprises several terranes: from north to south, the Songpan–Ganze, Qiangtang, Lhasa and Yangtze terranes, which were welded together prior to the Cretaceous to form part of the Eurasian plate (Fig. 1). From ca. 70–60 Ma, the Indo-Asian collision created the Tibetan plateau and resulted in northeastward extrusion tectonics facilitated by strike-slip motion along a series of strike-slip faults (such as Jiali fault, Batang–Lijiang fault, Gaoligong fault, etc.; Fig. 1), including the Jinshajiang–Red River deep fault. Strike-slip motion along the Jinshajiang–Red River deep fault caused lithospheric-scale extension and emplacement of numerous alkali-rich igneous rocks including volcanic and intrusive rocks, forming a >1500 km-long and generally 50–80 km-wide Jinshajiang–Red River alkali-rich magmatic belt (Bi, 1999; Chung et al., 1997, 1998; Hou et al., 2006, 2007c; Turner et al., 1996; Yin and Harrison, 2000; Zhang et al., 1987). K–Ar and Ar–Ar dating of whole-rock and mineral samples of feldspar and biotite indicate that these alkali-rich igneous rocks have ages ranging from ca. 41 Ma to 27 Ma (Zhang and Xie, 1997).

Geochemically, these alkali-rich igneous rocks range from basaltic to trachytic and rhyolitic in composition (Chung et al., 1998), and are characterized by high alkali ($K_2O + Na_2O > 8\%$ wt.) and enrichment in potassium ($K_2O/Na_2O > 1$), thus belonging to high-K calc-alkaline or shoshonitic series, and show incompatible trace-element patterns with highly enriched large-ion lithophile elements and light rare-earth elements, and marked depletions in the high field strength elements (HFSE) such as Nb, Ta and Ti (Bi et al., 2005; Chung et al., 1998; Hou et al., 2003). The Sr–Nd isotopic compositions of these alkali-rich igneous rocks (Bi et al., 2005; Hou et al., 2003; Jiang et al., 2006; Zhang and Xie, 1997) indicate that they originated from an enriched mantle source (EMII). The rock types of alkali-rich intrusions related to porphyry Cu–Mo mineralization mainly consist of monzogranite porphyry, syenogranite porphyry, granite porphyry, monzonite porphyry and syenite porphyry. The porphyry Cu–Mo deposits are all located at both the exo- and endo-contact zones of alkali-rich intrusions, and are controlled by fractures and faults (Hu et al., 2004).

According to the distribution of porphyry Cu–Mo deposits in major tectonic units, such as 1) the Ailaoshan–Red River strike-slip system, and 2) the Jinshajiang strike-slip fault system. The porphyry Cu–Mo mineralization in the Jinshajing–Red River belt mainly occurred in two secondary ore belts, one is the Ailaoshan–Red River porphyry Cu–Mo ore belt in southern segment of this belt, and the other is the Yulong porphyry Cu–Mo ore belt in northern segment of this belt (Fig. 1; Hou et al., 2003, 2007a).

2.1. Ailaoshan–Red River porphyry Cu–Mo ore belt

The Ailaoshan–Red River porphyry Cu–Mo ore belt extends for more than 1000 km from Dali in the north to the South China Sea in the south (Figs. 1 and 2). Four porphyry Cu–Mo deposits, including Machangqing (reserve of 0.25 Mt Cu at 0.44%), Habo (reserves of 0.53 Mt Cu at 0.42–1.0% and 37,718 t Mo at 0.01–0.1%), Tongchang (reserves of 8,621 t Cu at 1.24% and 17,060 t Mo at 0.218%) and Chang'anchong (reserves of 29,337 t Cu at 1.48% and 13,310 t Mo at 0.13%), have been discovered in the Ailaoshan–Red River ore belt (Hou et al., 2003, 2006; Xue, 2008; Zhu, 2010). Moreover, one

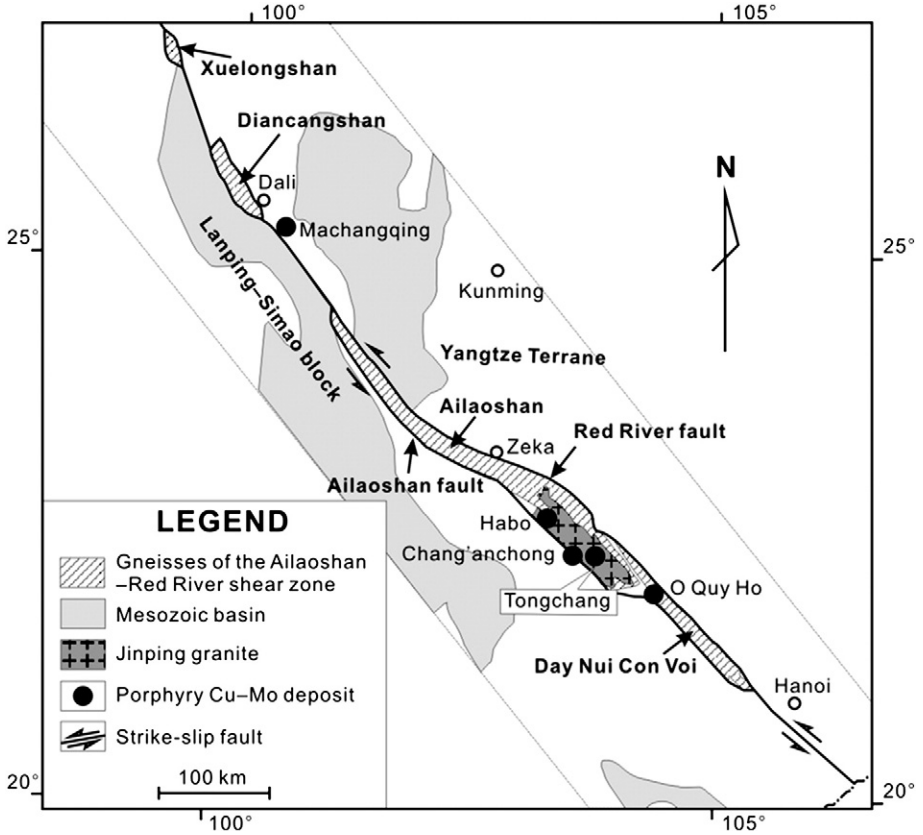

Fig. 2. Structural features and distribution of porphyry Cu–Mo deposits in the Ailaoshan–Red River ore belt (modified from Zhang and Schärer, 1999).

Table 1
Summary of geological and mineralization characteristics of some representative porphyry Cu–Mo deposits in the Jinshajiang–Red River porphyry Cu–Mo metallogenic belt.

Deposit	Location	Wall rock	Intrusion type	Occurrence	Outcrop area	Alteration	Mineralization	Mineralization scale (contained metals)	Ore grade	Ore structure	Shape of orebody
Yulong ore belt											
Narigongma[a]	Qinghai Province, China	P_{2-3}: basalt	Biotite granite porphyry	Stocks	0.96 km^2	Outward from center: K-silicate → quartz–sericite → propylitic → argillic	Cu–Mo–Au	0.25 Mt Cu, 0.675 Mt Mo	Cu: 0.33%, Mo: 0.079%	Veinlet	Stratiform and lenticular orebody in stock and contact
Yulong[b]	Tibet autonomous region, China	T_3: crystalline limestone	Monzogranite porphyry	Stocks	0.64 km^2	Outward from center: K-silicate → quartz–sericite → propylitic → argillic → skarn	Cu–Mo–Au	6.5 Mt Cu, 0.15 Mt Mo	Cu: 0.38%, Mo: 0.04%, Au: 0.35 ppm	Veinlet, disseminated, brecciated	Stratiform and lenticular orebody surrounding stock, pipe-like orebody
Zhanaga[c]	Tibet autonomous region, China	T_3: sandy mudstone	Monzogranite porphyry	Stocks	0.60 km^2	From south to north: K-silicate → quartz–sericite → propylitic → argillic → skarn	Cu–Mo–Au	0.30 Mt Cu, Mo?	Cu: 0.36%, Mo: 0.03%, Au: 0.03 ppm	Veinlet, disseminated	Pipe-like orebody in stock
Mangzong[c]	Tibet autonomous region, China	T_3: sandy mudstone	Monzogranite porphyry	Stocks	0.28 km^2	Outward from center: K-silicate → quartz–sericite → propylitic → skarn	Cu–Mo–Au	0.25 Mt Cu, Mo?	Cu: 0.34%, Mo: 0.03%, Au: 0.02 ppm	Veinlet, disseminated	Regular pipe-like orebody in stock
Duoxiasongduo[c]	Tibet autonomous region, China	T_3: sandy mudstone	Monzogranite porphyry	Stocks	0.30 km^2	Outward from center: K-silicate → quartz–sericite → propylitic → skarn	Cu–Mo–Au	0.50 Mt Cu, Mo?	Cu: 0.38%, Mo: 0.04%, Au: 0.05 ppm	Veinlet, disseminated, stockwork	Regular lenticular orebody in stock
Malasongduo[c]	Tibet autonomous region, China	T_1: rhyolite	Monzogranite porphyry	Stocks	0.13 km^2	Outward from center: K-silicate → quartz–sericite → propylitic → skarn	Cu–Mo–Au	1.0 Mt Cu, Mo?	Cu: 0.44%, Mo: 0.14%, Au: 0.06 ppm	Veinlet, disseminated	Regular lenticular orebody in stock
Ailaoshan–Red River ore belt											
Machangqing[c]	Yunan Province, China	O_1–D_1: limestone and sandstone	Granite porphyry	Stocks	1.3 km^2	Outward from center: K-silicate → sericite → advanced argillic → skarn	Cu–Mo–Au	0.25 Mt Cu, Mo?	Cu: 0.44%, Mo: 0.14%, Au: 0.06 ppm	Veinlet, disseminated, massive	Lenticular, pocket, and irregular orebody in stock
Habo[d]	Yunan Province, China	Hymalayan granite	Biotite quartz monzonite porphyry, quartz monzonite porphyry, monzonite porphyry	Stocks and dykes	>1.0 km^2	Outward from center: K-silicate → quartze–sericite → propylitic	Cu–Mo–Au	0.53 Mt Cu, 37718 t Mo	Cu: 0.42–1.0%, Mo: 0.01–0.1%, Au: 1–33 ppm	Veinlet, disseminated	Stratiform and lenticular orebody in stock and contact
Tongchang[e]	Yunan Province, China	S_2: dolomitic limestone and sandstone	Quartz syenite porphyry	Stocks and dykes	0.20 km^2	Outward from center: K-silicate → quartz–sericite → skarn	Cu–Mo–Au	8621 t Cu, 17060 t Mo	Cu: 1.24%, Mo: 0.218%, Au: 0.13 ppm	Veinlet, disseminated, massive	Stratiform and lenticular orebody in stock and skarn
Chang'anchong[e]	Yunan Province, China	S_2: dolomitic limestone and sandstone	Quartz syenite porphyry	Stocks	>0.18 km^2	Outward from center: K-silicate → quartz–sericite → skarn	Cu–Mo–Au	29337 t Cu, 13310 t Mo	Cu: 1.48%, Mo: 0.13%, Au: 0.25 ppm	Veinlet, disseminated, massive	Stratiform and lenticular orebody in stock and skarn
O Quy Ho[f]	Lao Cai Province, Vietnam	Proterozoic graphite schist and garnet biotite schist, Mesozoic biotite granite	Hornblende granite porphyry	Stocks and dykes	>2.5 km^2	K-feldspar, sericite, quartz–K-feldspar	Cu–Mo	16000 t Mo; Cu?	Mo: 0.2%	Veinlet, disseminated	Stratiform and lenticular orebody in stock and wall-rock

[a] Wang et al. (2008), Yang et al. (2008).
[b] Liang et al. (2008).
[c] Hou et al. (2003, 2006).
[d] Zhu (2010).
[e] Xue (2008).
[f] Tran et al. (2010).

porphyry Mo deposit in Vietnam, O Quy Ho, with a reserve of 16,000 t Mo (at 0.2%) is regarded as part of the Ailaoshan–Red River ore belt (Figs. 1 and 2; Tran et al., 2010).

The Cu–Mo-mineralized alkali-rich porphyries in the Ailaoshan–Red River belt are all felsic, with SiO_2 ranging from 65.0 to 70.0 wt.%, K_2O+Na_2O from 8.1 to 11.1 wt.%, $K_2O/Na_2O>1$, high I_{sr} (0.7053–0.7073) and low $\varepsilon_{Nd}(t)$ (−10.4–−3.4) (Xu, 2011). Lithologically, the Cu–Mo-mineralized rocks are mostly composed of granite porphyry in the Machangqing and O Quy Ho deposits, monzonite porphyry in the Habo deposit and syenite porphyry in the Tongchang and Chang'anchong deposits. Geological and mineralization features of these deposits are summarized in Table 1.

The porphyry Cu–Mo deposits in the Ailaoshan–Red River ore belt are mainly distributed along the NW-trending Ailaoshan–Red River (ASRR) shear zone. The ASRR shear zone is bordered to the east by the Red River deep fault marking the boundary with the Yangtze Terrane, and to the west by the Ailaoshan deep fault abutting the Lanping–Simao block (Figs. 1 and 2). Although currently active, with right-lateral slip and normal throw (Allen et al., 1984; Replumaz et al., 2001; Tapponnier and Molnar, 1977), the ASRR shear zone was a left-lateral strike-slip fault that allowed the Indochina block to move southeastward in response to the Indo-Asian collision during the Tertiary (Fig. 1; Peltzer and Tapponnier, 1988; Tapponnier et al., 1982, 1986). Geological evidence suggests that the total left-lateral offset along the ASRR shear zone is >700 km (Chung et al., 1997; Lacassin et al., 1996; Leloup et al., 1993, 1995, 2001; Sato et al., 1999; Yang et al., 1995).

2.2. Yulong porphyry Cu–Mo ore belt

The Yulong porphyry Cu–Mo ore belt is >400 km long and 15–30 km wide. Six porphyry Cu–Mo deposits including Narigongma (reserves of 0.25 Mt Cu at 0.33% and 0.675 Mt Mo at 0.079%), Yulong (reserves of 6.5 Mt Cu at 0.38% and 0.15 Mt Mo at 0.04%), Malasongduo (reserve of 1.0 Mt Cu at 0.44%), Duoxiasongduo (reserve of 0.50 Mt Cu at 0.38%), Zhanaga (reserve of 0.30 Mt Cu at 0.36%) and Mangzong (reserve of 0.25 Mt Cu at 0.34%) (Table 1), and more than 20 Cu–Mo-porphyry prospects have been identified in this belt, with a total resource of Cu and Mo exceeding 10 Mt (Figs. 1 and 3; Hou et al., 2003; Liang et al., 2008).

Mineralized Cu–Mo alkali-rich porphyries in the Yulong belt are all felsic, with SiO_2 mainly around 70.0 wt.%, K_2O+Na_2O from 7.8 to 9.4 wt.%, $K_2O/Na_2O>1$, high I_{sr} (0.7048–0.7077) and relatively high $\varepsilon_{Nd}(t)$ (−2.8–0.7) (Hou et al, 2003; Jiang et al., 2006; Yang et al., 2008). Lithologically, the Cu–Mo-mineralized rocks mainly consist of monzogranite porphyry in the Yulong, Zhanaga, Mangzong, Duoxiasongduo and Malasongduo deposits, and granite porphyry in the Narigongma deposit. Geological and mineralization features of these deposits in the Yulong belt are summarized in Table 1.

The Yulong belt is tectonically located in the Changdu Block, a Mesozoic sedimentary basin, to the eastern part of the Tibetan plateau (Fig. 3). The Yulong ore belt is mainly distributed along the Jinshajiang right-lateral strike-slip deep fault system consisting of the Chesuo and Wenquan strike-slip faults. The strike-slip faults resulted in the formation of the Gonjo strike-slip pull-apart basin, filled up with >4000 m-thick Tertiary red molasse accumulations, and alkali-rich volcanic rocks. The host porphyries of the Yulong porphyry Cu–Mo ore belt are mainly controlled by a set of the secondary NNW-directed strike-slip faults and folds derived from the Wenquan right-lateral strike-slip faulting (Fig. 3; Hou et al., 2003, 2007a).

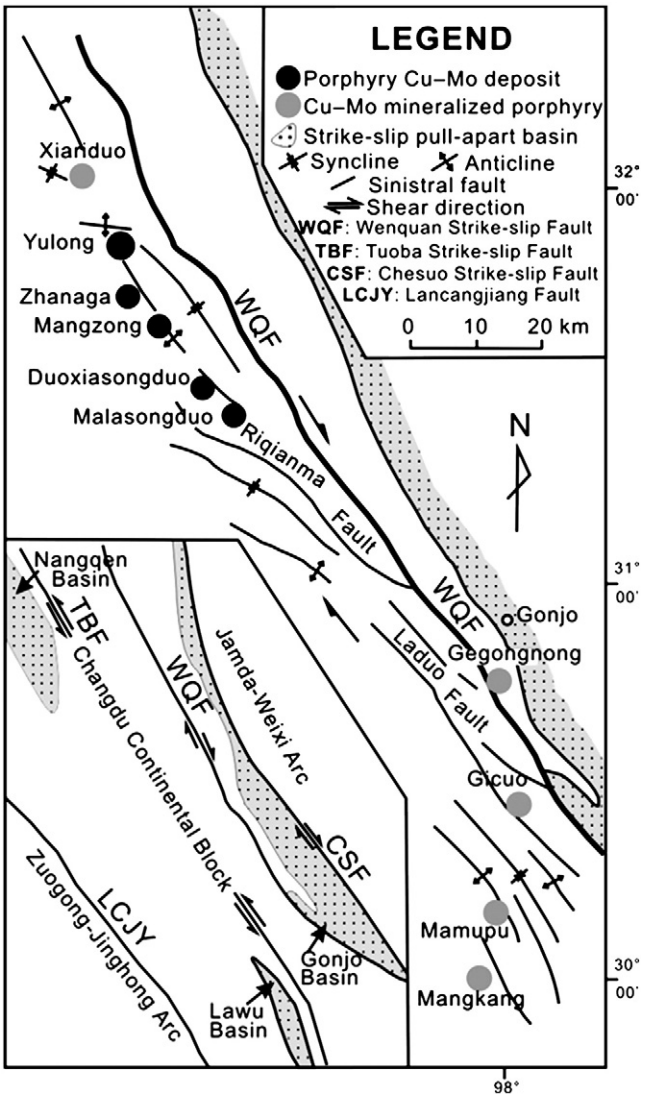

Fig. 3. Structural features and distribution of porphyry Cu–Mo deposits in the Yulong ore belt (modified from Hou et al., 2007a).

3. Sampling and analytical methods

3.1. Zircon LA-ICPMS U–Pb dating

Four rock samples, from the Tongchang, Chang'anchong, Machangqing and Yulong porphyry Cu–Mo deposits, respectively, were collected for zircon separation. Zircon grains were separated from ~2 kg of rock using standard density and magnetic separation techniques. Representative grains were hand-picked and mounted in an epoxy resin disk, and then polished. Internal structure was examined using cathodoluminescence (CL) prior to U–Pb isotopic analysis. Cathodoluminescence imaging was done using a Quanta 400FEG environmental scanning electron microscope equipped with an Oxford energy dispersive spectroscopy system and a Gatan CL3+ detector at the State Key Laboratory of Continental Dynamics, Northwest University, Xi'an, China. The operating conditions for the CL imaging were 15 kV and 20 nA.

Zircon U–Pb analyses were performed using the laser-ablation, inductively coupled plasma mass spectrometer (LA-ICPMS) at the State Key Laboratory of Geological Processes and Mineral Resources, China University of Geosciences, Wuhan, China. A pulsed (Geolas) 193 nm ArF Excimer (Lambda Physik, Göttingen Germany) laser power of 50 mJ/pulse energy was used for ablation, at a repetition rate of 10 Hz. The diameter of the laser spot was 32 μm. The detailed analytical procedures follow those described by Liu et al. (2008, 2010a,b). Helium is advantageous as a carrier gas. Argon was used as the make-up gas and mixed with the carrier gas via a T-connector before entering the ICP. Harvard zircon 91500 was used as an external standard to normalize isotopic fractionation during analysis. The NIST610

glass was used as an external standard to calculate U, Th, and Pb concentrations of unknowns. An Agilent 7500a ICP-MS instrument was used to acquire ion-signal intensities. Each analysis incorporated a background acquisition of approximately 20–30 s (gas blank) followed by 50 s data acquisition from the sample. Off-line selection and integration of background and analyte signals, and time-drift correction and quantitative calibration for U–Pb dating were performed by ICPMSDataCal (Liu et al., 2010a,b). A common Pb correction was

Table 2
Zircon U–Pb isotopic data obtained by LA-ICPMS for Tongchang quartz syenite porphyry, Chang'anchong quartz syenite porphyry, Machangqing granite porphyry and Yulong monzogranite porphyry.

Spot	Th (ppm)	U (ppm)	Th/U	$^{207}Pb/^{235}U$	1σ	$^{206}Pb/^{238}U$	1σ	$^{207}Pb/^{206}Pb$	1σ	$^{206}Pb/^{238}U$ (Ma)	1σ
Tongchang (sample TC920)											
1	463	1077	0.43	0.03530	0.00223	0.00556	0.00005	0.04605	0.00294	35.7	0.3
2	405	1144	0.35	0.03523	0.00212	0.00555	0.00007	0.04605	0.00283	35.7	0.4
3	484	1150	0.42	0.03580	0.00190	0.00562	0.00006	0.04682	0.00259	36.2	0.4
4	668	1349	0.49	0.03461	0.00205	0.00545	0.00005	0.04606	0.00276	35.0	0.3
5	441	1116	0.39	0.03543	0.00181	0.00551	0.00006	0.04728	0.00240	35.4	0.4
6	861	1396	0.62	0.03681	0.00171	0.00550	0.00006	0.04890	0.00227	35.3	0.4
7	422	1017	0.41	0.03780	0.00199	0.00565	0.00006	0.04882	0.00267	36.3	0.4
8	675	1378	0.49	0.03594	0.00166	0.00561	0.00005	0.04639	0.00222	36.1	0.3
9	700	1318	0.53	0.03575	0.00151	0.00559	0.00005	0.04673	0.00205	36.0	0.3
10	471	1140	0.41	0.03592	0.00160	0.00564	0.00006	0.04638	0.00211	36.3	0.4
11	644	1170	0.55	0.03563	0.00091	0.00561	0.00005	0.04605	0.00124	36.1	0.3
12	449	1108	0.41	0.03607	0.00181	0.00557	0.00006	0.04728	0.00243	35.8	0.4
13	500	1227	0.41	0.03795	0.00194	0.00558	0.00006	0.04889	0.00242	35.9	0.4
14	457	1114	0.41	0.03730	0.00170	0.00551	0.00005	0.04934	0.00233	35.4	0.3
Chang'anchong (sample CA910)											
1	385	826	0.47	0.04698	0.00376	0.03772	0.00298	0.00582	0.00008	37.4	0.5
2	424	303	1.40	0.04606	0.00802	0.03525	0.00611	0.00555	0.00010	35.7	0.6
3	436	809	0.54	0.04766	0.00466	0.03749	0.00351	0.00575	0.00007	37.0	0.5
4	537	1165	0.46	0.04608	0.00311	0.03545	0.00242	0.00563	0.00007	36.2	0.4
5	392	826	0.47	0.04902	0.00428	0.03758	0.00324	0.00573	0.00007	36.9	0.5
6	549	1132	0.48	0.04656	0.00271	0.03576	0.00204	0.00564	0.00006	36.2	0.4
7	635	1174	0.54	0.04584	0.00252	0.03503	0.00191	0.00563	0.00007	36.2	0.4
8	546	1029	0.53	0.04605	0.00199	0.03579	0.00151	0.00564	0.00006	36.2	0.4
9	357	743	0.48	0.04998	0.00365	0.03832	0.00277	0.00577	0.00007	37.1	0.4
10	412	812	0.51	0.04816	0.00474	0.03697	0.00360	0.00557	0.00007	35.8	0.5
11	582	978	0.60	0.04737	0.00282	0.03583	0.00208	0.00560	0.00006	36.0	0.4
12	638	1164	0.55	0.04963	0.00282	0.03724	0.00201	0.00558	0.00006	35.9	0.4
13	473	958	0.49	0.04770	0.00342	0.03627	0.00261	0.00561	0.00007	36.1	0.4
14	510	865	0.59	0.04970	0.00441	0.03732	0.00324	0.00565	0.00008	36.3	0.5
Machangqing (sample LDS906)											
1	850	928	0.92	0.04800	0.00195	0.03790	0.00153	0.00571	0.00006	36.7	0.4
2	1007	1092	0.92	0.05043	0.00190	0.03919	0.00143	0.00566	0.00006	36.4	0.4
3	1513	899	1.68	0.05101	0.00218	0.03931	0.00165	0.00558	0.00006	35.9	0.4
4	1864	951	1.96	0.05072	0.00186	0.03918	0.00141	0.00562	0.00006	36.1	0.4
5	585	1041	0.56	0.04793	0.00178	0.03675	0.00135	0.00557	0.00005	35.8	0.3
6	463	1048	0.44	0.04954	0.00200	0.03866	0.00151	0.00568	0.00006	36.5	0.4
7	313	720	0.43	0.04606	0.00235	0.03521	0.00176	0.00554	0.00005	35.6	0.3
8	1019	1206	0.84	0.04515	0.00159	0.03521	0.00116	0.00570	0.00006	36.7	0.4
9	354	742	0.48	0.04727	0.00210	0.03638	0.00159	0.00561	0.00006	36.1	0.4
10	588	1039	0.57	0.04645	0.00191	0.03662	0.00151	0.00574	0.00005	36.9	0.3
11	569	934	0.61	0.04811	0.00205	0.03663	0.00153	0.00552	0.00005	35.5	0.3
12	2003	1964	1.02	0.04753	0.00145	0.03647	0.00111	0.00556	0.00004	35.7	0.3
13	433	861	0.50	0.04864	0.00205	0.03825	0.00167	0.00568	0.00006	36.5	0.4
14	470	910	0.52	0.04998	0.00213	0.03916	0.00161	0.00574	0.00006	36.9	0.4
15	350	707	0.49	0.05047	0.00228	0.03941	0.00173	0.00571	0.00006	36.7	0.4
16	403	655	0.61	0.04959	0.00354	0.03829	0.00269	0.00560	0.00007	36.0	0.4
Yulong (sample YL912)											
1	584	1210	0.48	0.04782	0.00160	0.04315	0.00161	0.00659	0.00014	42.3	0.9
2	672	1324	0.51	0.04880	0.00166	0.04282	0.00158	0.00648	0.00016	42.0	1.0
3	1182	1219	0.97	0.04761	0.00172	0.04331	0.00166	0.00662	0.00013	42.6	0.8
4	654	1250	0.52	0.04881	0.00170	0.04471	0.00160	0.00675	0.00014	43.4	0.9
5	388	983	0.39	0.05044	0.00190	0.04638	0.00165	0.00682	0.00013	43.8	0.8
6	996	1178	0.85	0.04675	0.00177	0.04297	0.00162	0.00681	0.00013	43.7	0.9
7	692	704	0.98	0.05036	0.00220	0.04602	0.00222	0.00666	0.00014	42.8	0.9
8	719	1231	0.58	0.04737	0.00154	0.04415	0.00151	0.00678	0.00010	43.6	0.7
9	458	1237	0.37	0.04653	0.00148	0.04274	0.00135	0.00671	0.00009	43.1	0.6
10	980	1444	0.68	0.04768	0.00154	0.04391	0.00139	0.00668	0.00005	42.9	0.3
11	367	878	0.42	0.04832	0.00179	0.04474	0.00156	0.00676	0.00007	43.4	0.4
12	439	1018	0.43	0.04642	0.00180	0.04225	0.00158	0.00668	0.00007	42.9	0.5
13	572	1308	0.44	0.04796	0.00119	0.04456	0.00110	0.00673	0.00005	43.3	0.3
14	897	1427	0.63	0.04946	0.00144	0.04573	0.00127	0.00671	0.00006	43.1	0.4
15	1254	1171	1.07	0.04713	0.00145	0.04376	0.00135	0.00675	0.00006	43.4	0.4

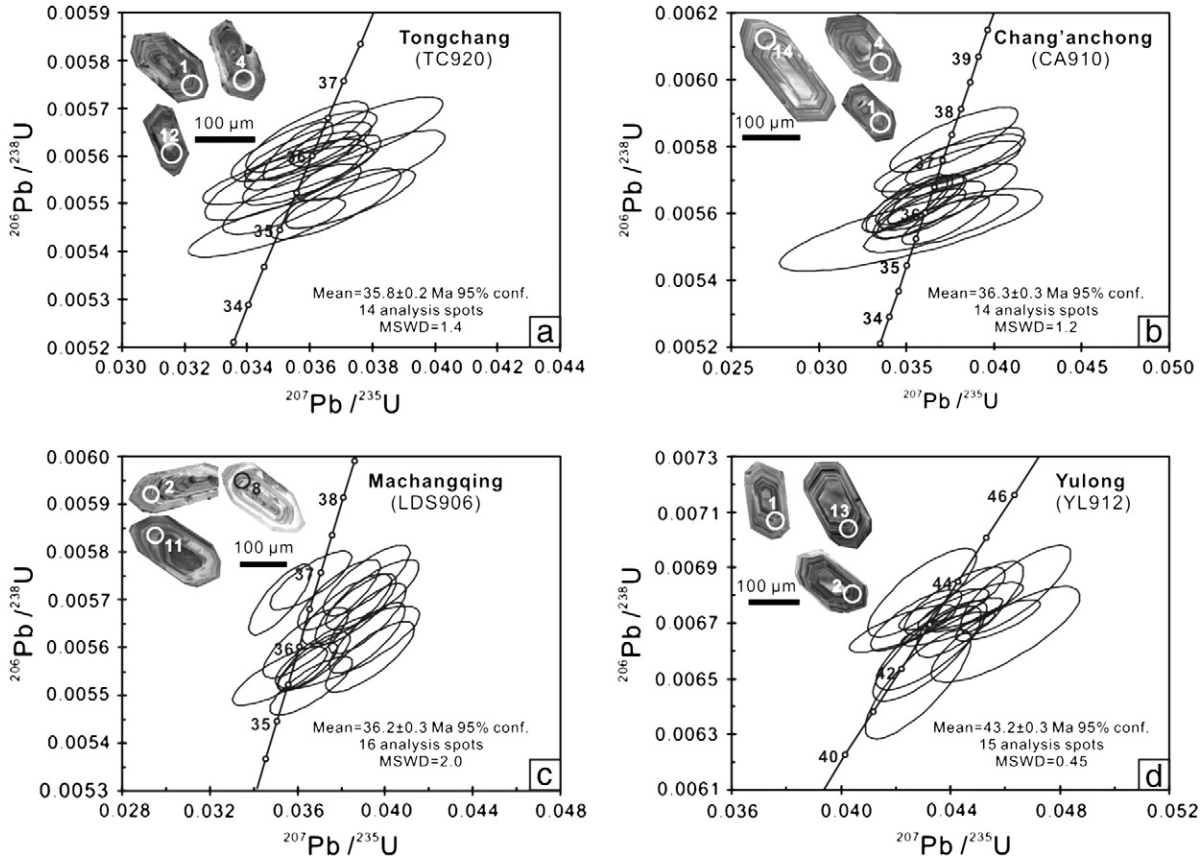

Fig. 4. Zircon U–Pb concordia diagrams for Tongchang host quartz syenite porphyry (a), Chang'anchong host quartz syenite porphyry (b), Machangqing host granite porphyry (c) and Yulong host monzogranite porphyry (d).

applied using the method of Andersen (2002), which has minimal effect on the age results. Uncertainties of individual analyses are reported with 1σ errors; weighted mean ages were calculated at 2σ confidence level. Concordia diagrams and weighted mean age calculations were made using the ISOPLOT 2.49 program of Ludwig (2001).

3.2. Molybdenite Re–Os dating

Molybdenite samples were collected from the K-silicate and quartz-sericite alteration zones of Tongchang and Chang'anchong porphyry Cu–Mo deposits, respectively. Molybdenite separates were obtained through following procedures. Firstly, ore samples were crushed to fine particles. Then particles of 40–60 mesh were obtained by sieving. Then molybdenite concentrates were separated from 40 to 60 mesh particles by heavy liquid techniques. The molybdenite separates were handpicked under a binocular microscope in order to remove impurities of the concentrates. The ^{187}Re and ^{187}Os concentrations in 0.02–0.05 g molybdenite aliquots were determined at the Re–Os Laboratory, National Research Center of Geoanalysis (Beijing). Details of the chemical separating process and ICP-MS analysis of Re and Os isotopes are given by Du et al. (1994, 2001) and Qu and Du (2003). A brief description is given below.

A Carius tube digestion method was used. The weighed sample was loaded in a Carius tube through a thin neck long funnel. The mixed ^{185}Re and ^{190}Os spike and 2 ml of 10 mol/l HCl, 4 ml of 16 mol/l HNO3, and

Table 3
Re–Os isotopic data of molybdenite for Tongchang and Chang'anchong porphyry Cu–Mo deposits.

Deposit	Sample	Weight (g)	Total Re (μg/g)	Common Os (ng/g)	^{187}Re (ng/g)	^{187}Os (ng/g)	Model age (Ma)
Tongchang	TC801	0.03011	29.77 (0.24)	0.0263 (0.0215)	18710 (150)	10.53 (0.10)	33.8 (0.5)
	TC811	0.03061	33.83 (0.25)	0.0360 (0.0261)	21260 (160)	12.22 (0.10)	34.5 (0.5)
	TC814	0.03054	13.32 (0.10)	0.1148 (0.0053)	8375 (62)	4.786 (0.044)	34.3 (0.5)
	TC817	0.03035	74.39 (0.59)	0.0152 (0.0210)	46760 (370)	26.71 (0.22)	34.3 (0.5)
	TC907	0.02087	107.3 (1.0)	0.0430 (0.0158)	67440 (640)	38.47 (0.34)	34.2 (0.5)
	TC926	0.03092	76.87 (0.65)	0.0668 (0.0156)	48320 (410)	27.89 (0.23)	34.6 (0.5)
	TC927	0.03030	21.84 (0.18)	0.0474 (0.0107)	13730 (120)	7.848 (0.062)	34.3 (0.5)
	TC929	0.03035	134.7 (1.1)	0.0567 (0.0104)	84650 (680)	47.3 (0.37)	33.5 (0.5)
	TC930	0.03001	157.1 (1.1)	0.0634 (0.0214)	98760 (720)	56.46 (0.46)	34.3 (0.5)
Chang'anchong	CA903	0.10086	7.455 (0.064)	0.0313 (0.0007)	4686 (40)	2.675 (0.023)	34.3 (0.5)
	CA937	0.00558	374.8 (2.9)	1.7143 (0.0667)	235500 (1800)	136.2 (1.2)	34.7 (0.5)
	CA940	0.10018	36.15 (0.32)	0.0622 (0.0033)	22720 (200)	12.95 (0.10)	34.2 (0.5)
	CA943	0.10022	105.1 (0.90)	0.0498 (0.0039)	66040 (570)	36.73 (0.31)	33.4 (0.5)
	CA944	0.10018	41.44 (0.50)	0.0283 (0.0032)	26040 (320)	14.74 (0.12)	34.0 (0.6)
	CA945	0.10025	126.3 (1.8)	0.0554 (0.0033)	79370 (1100)	44.56 (0.36)	33.7 (0.6)
	CA948	0.02020	7.139 (0.054)	0.0433 (0.0119)	4487 (34)	2.637 (0.024)	35.3 (0.5)

Values in parenthesis are absolute uncertainties (2σ). Uncertainties in ages are calculated using error propagation and include errors in the ^{185}Re and ^{190}Os spike calibration, the Re decay constant, and spectroscopic measurements. Model age and isochron age were calculated using Isoplot (Ludwig, 2001). Uncertainties for ages are absolute (2σ).

1 ml of 30% H_2O_2 were loaded while the bottom part of the tube was frozen at −80 to −50 °C in an ethanol–liquid nitrogen slush; the top was sealed using an oxygen–propane torch. The tube was then placed in a stainless steel jacket and heated for 24 h at 200 °C. Upon cooling, the bottom part of the tube was kept frozen, the neck of the tube was broken, and the contents of the tube were poured into a distillation flask and the residue was washed out with 40 ml of water.

OsO_4 was distilled at 105–110 °C for 50 min and trapped in 10 ml of water. The residual Re-bearing solution was saved in a 150-ml Teflon beaker for Re separation. The Os isotope ratio was determined using an inductively coupled plasma mass spectrometer (TJA X-series ICP-MS).

The Re-bearing solution was evaporated to dryness; 1 ml of water was added, and then the solution was evaporated to near dryness twice. 10 ml of 5 mol/l NaOH was added to the residue followed by Re extraction with 10 ml acetone in a 120-ml Teflon separation funnel. The water phase was then discarded and the acetone phase washed with 2 ml of 5 mol/l NaOH. The acetone phase was transferred to a 150-ml beaker that contained 2 ml of water. After evaporation to dryness, several (2–3) drops of concentrated nitric acid (~15 mol/l) and several (2–3) drops of H_2O_2 (30%) were added to the beaker followed by evaporating to dryness to remove the residual osmium. Several ml of dilute nitric acid (~2%) were added for dissolving the residue. The Re isotope ratio was determined using the inductively coupled plasma mass spectrometer (TJA X-series ICP-MS). If the salinity of the Re-bearing solution was more than 1 mg/ml, the Na was removed using cation-exchange resin (Du et al., 1994).

The molybdenite standard GBW04436 (JDC) used in this study gave a mean value of 139.2 ± 2.8 Ma, which is in agreement with the certified value of 139.6 ± 3.8 Ma (Du et al., 2004). Blanks during this study were 0.0613–0.0802 ng for Re and 0.0002–0.0003 ng for Os. The Re–Os isochron age was calculated by using the least-squares method of York (1969), as implemented in the ISOPLOT 2.49 program (Ludwig, 2001). The age calculation is using a ^{187}Re decay constant of 1.666×10^{-11} (Smoliar et al., 1996). Uncertainty in Re–Os model ages includes 1.02% uncertainty in the ^{187}Re decay constant and uncertainty in Re and Os concentrations which comprises weighing error for both spike and sample, uncertainty in spike calibration and mass spectrometry analytical error.

4. Results

4.1. Zircon LA-ICPMS U–Pb age data

Zircon LA-ICPMS U–Pb analytical results for the Tongchang quartz syenite porphyry, Chang'anchong quartz syenite porphyry, Machangqing granite porphyry and Yulong monzogranite porphyry are listed in Table 2 and illustrated on a concordia plot in Fig. 4. The analyzed zircons are mostly clear and idiomorphic crystals with magmatic oscillatory zoning (Fig. 4).

Zircon grains of the Tongchang quartz syenite porphyry (Sample TC920) have high and uniform concentrations of U and Th (1017–1396 and 405–861 ppm, respectively). Their Th/U ratios (0.35–0.62) are typical of magmatic genetic origin. These zircon grains yield concordant to nearly concordant U–Pb ages. 14 analyses have $^{206}Pb/^{238}U$ ages of 35.0 to 36.3 Ma with a mean $^{206}Pb/^{238}U$ age of 35.8 ± 0.2 Ma (2σ, MSWD = 1.4) (Fig. 4a).

Zircon grains of the Chang'anchong quartz syenite porphyry (Sample CA910) contain 303–1174 ppm U and 357–639 ppm Th. Most analyzed zircon grains have Th/U ratios of typical magmatic origin (mostly 0.46–0.60), apart from 1 analysis (Spot 2) with a higher ratio of 1.40. These zircon grains are concordant to nearly concordant, and have $^{206}Pb/^{238}U$ ages ranging from 35.7 to 37.4 Ma, and yield a mean $^{206}Pb/^{238}U$ age of 36.3 ± 0.3 Ma (2σ, MSWD = 1.2) (Fig. 4b).

Zircon grains of the Machangqing granite porphyry (Sample LDS906) have a wide range of U (655–1964 ppm) and Th (313–2003 ppm). Three

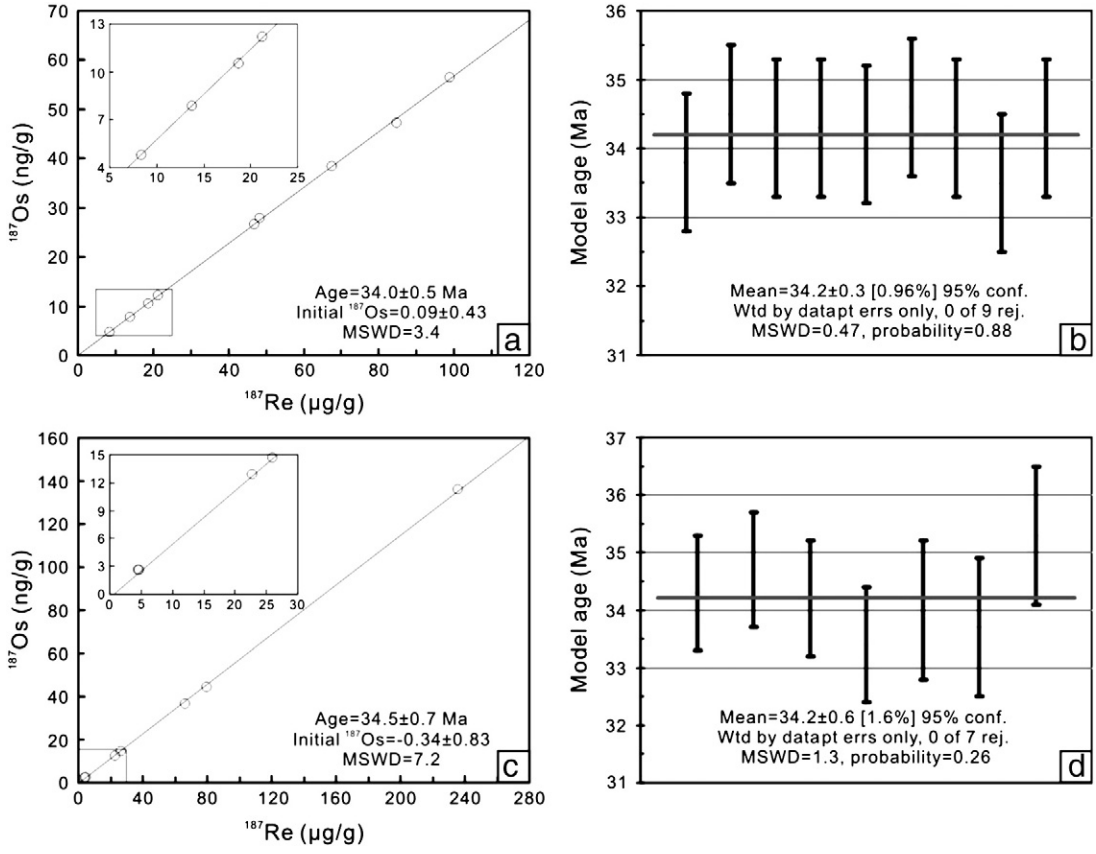

Fig. 5. Molybdenite Re–Os isochrons and weighted mean model ages for Tongchang (a and b) and Chang'anchong (c and d) porphyry Cu–Mo deposits.

analyses (Spot 2, 4 and 12) have high Th/U ratios of >1.0, the rest show Th/U ratios of typical magmatic origin (mostly 0.43–0.92). All 16 zircon grains analyzed are concordant to nearly concordant and yield a mean $^{206}Pb/^{238}U$ age of 36.2 ± 0.3 Ma (2σ, MSWD = 2.0) (Fig. 4c).

Zircon grains of the Yulong monzogranite porphyry (Sample YL912) have 704–1444 ppm of U and 367–1254 ppm of Th. Most analyses show Th/U ratios (mostly 0.43–0.92) of typical magmatic genetic zircon except 1 analysis (Spot 15) with Th/U ratios of slightly >1.0. All 15 zircon grains analyzed are concordant to nearly concordant and yield a mean $^{206}Pb/^{238}U$ age of 43.2 ± 0.3 Ma (2σ, MSWD = 0.45) (Fig. 4d).

4.2. Molybdenite Re–Os dating

Re–Os isotopic analytical results of 16 molybdenite samples from the Tongchang and Chang'anchong porphyry Cu–Mo deposits are listed in Table 3. The Re–Os isochrons and weighted mean model ages of molybdenite from the Tongchang and Chang'anchong porphyry Cu–Mo deposits are plotted in Fig. 5.

Nine molybdenite samples from the Tongchang porphyry Cu–Mo deposit yield model ages ranging from 34.6 Ma to 33.5 Ma, with a well-defined ^{187}Re–^{187}Os isochron age of 34.0 ± 0.5 Ma (MSWD = 3.4) (Fig. 5a) and a weighted mean model age of 34.2 ± 0.3 Ma (MSWD = 0.47) (Fig. 5b). The intercept value of 0.09 ± 0.43 on the ^{187}Os axis for isochrone is nearly zero within uncertainty, which is expected because molybdenite contains little or no non-radiogenic ^{187}Os. This indicates that the model age measured with the contents of ^{187}Re and ^{187}Os in molybdenite is reliable (Selby and Creaser, 2001; Stein et al., 1997), and can be calculated with the equation: $t = (1/\lambda) \times \ln(1 + {}^{187}Os/{}^{187}Re)$. Moreover, the consistency between the isochron age and weighted mean model age within uncertainty indicates the analytical result is very believable.

Seven molybdenite samples from the Chang'anchong porphyry Cu–Mo deposit plot along a linear array on the isochron diagram and yield a well-constrained ^{187}Re–^{187}Os isochron age of 34.5 ± 0.7 Ma (MSWD = 7.2) (Fig. 5c), which is well consistent with the weighted mean model age of 34.2 ± 0.6 Ma (MSWD = 1.3) within uncertainty, calculated from model ages ranging from 35.3 Ma to 33.4 Ma, (Fig. 5d). The very small initial ^{187}Os value reflects that the model age measured with the contents of ^{187}Re and ^{187}Os in molybdenite is reliable (Selby and Creaser, 2001; Stein et al., 1997), and can be calculated with the equation: $t = (1/\lambda) \times \ln(1 + {}^{187}Os/{}^{187}Re)$.

5. Discussion

5.1. Geochronology of porphyry Cu–Mo deposits in the Jinshajiang–Red River belt

Zircon U–Pb and molybdenite Re–Os ages are critical for distinguishing magmatism and mineralization events, which can give the

Table 4
Summary of zircon U–Pb and molybdenite Re–Os age data of porphyry Cu–Mo deposits in the Jinshajiang–Red River porphyry Cu–Mo metallogenic belt.

Deposit	Location	Sampling site	Rock type	Analyzed phase	Method	Age (Ma)	Reference
Yulong ore belt							
Narigongma	Qinghai Province, China	Rock body	Biotite granite porphyry	Zircon	SHRIMP U–Pb	43.3 ± 0.5	Yang et al., 2008
		Orebody	Porphyry Cu–Mo orebody	Molybdenite	Re–Os	40.9 ± 0.9 (I)	Wang et al., 2008
Yulong	Tibet autonomous region, China	Rock body	Monzogranite porphyry	Zircon	SHRIMP U–Pb	40.9 ± 0.1	Liang, 2002
						38.9 ± 0.8	Jiang et al., 2006
						41.0 ± 1.0	Guo et al., 2006
					LA-ICPMS U–Pb	41.2 ± 0.3	Liang et al., 2006a
						41.3 ± 0.2	Liang et al., 2008
					SHRIMP U–Pb	43.0 ± 0.5	Wang et al., 2009
						43.8 ± 0.7	
					LA-ICPMS U–Pb	43.2 ± 0.3	this study
		Orebody	Porphyry Cu–Mo orebody	Molybdenite	Re–Os	40.1 ± 1.8 (I)	Hou et al., 2006
						41.6 ± 1.4 (I)	Tang et al., 2009
Zhanaga	Tibet autonomous region, China	Rock body	Monzogranite porphyry	Zircon	LA-ICPMS U–Pb	38.5 ± 0.2	Liang et al., 2006a
Mangzong	Tibet autonomous region, China					37.6 ± 0.2	
Duoxiasongduo	Tibet autonomous region, China					37.5 ± 0.2	
		Orebody	Porphyry Cu–Mo orebody	Molybdenite	Re–Os	36.0 ± 0.4 (M)	Du et al., 1994
Malasongduo	Tibet autonomous region, China	Rock body	Monzogranite porphyry	Zircon	LA-ICPMS U–Pb	37.1 ± 0.2	Liang et al., 2006a
						36.9 ± 0.4	Liang et al., 2009a,b
		Orebody	Porphyry Cu–Mo orebody	Molybdenite	Re–Os	35.9 ± 0.9 (W)	Tang and Luo, 1995
						35.8 ± 0.4 (W)	Du et al., 1994
Ailaoshan–Red River ore belt							
Machangqing	Yunan Province, China	Rock body	Granite porphyry	Zircon	SHRIMP U–Pb	35.0 ± 0.2	Liang et al., 2004
					LA-ICPMS U–Pb	36.2 ± 0.4	Wu et al., 2010
						36.2 ± 0.3	this study
		Orebody	Porphyry Cu–Mo orebody	Molybdenite	Re–Os	33.9 ± 1.1 (I)	Wang et al., 2004
						35.8 ± 1.6 (I)	Hou et al., 2006
						35.3 ± 0.7 (M)	Xing et al., 2009
						34.7 ± 0.5 (M)	He et al., 2011
Habo	Yunan Province, China	Rock body	Biotie quartz monzonite porphyry	Zircon	LA-ICPMS U–Pb	36.2 ± 0.2	Zhu, 2010
			Quartz monzonite porphyry			36.2 ± 0.2	
		Orebody	Porphyry Cu–Mo orebody	Molybdenite	Re–Os	35.5 ± 0.2 (M)	
Tongchang	Yunan Province, China	Rock body	Quartz syenite porphyry	Zircon	LA-ICPMS U–Pb	34.6 ± 0.2	Liang et al., 2002
						35.1 ± 0.3	Huang et al., 2009
						35.8 ± 0.2	this study
		Orebody	Porphyry Cu–Mo orebody	Molybdenite	Re–Os	34.4 ± 0.5 (I)	Wang et al., 2004
						34.0 ± 0.5 (I)	this study
Chang'anchong	Yunan Province, China	Rock body	Quartz syenite porphyry	Zircon	LA-ICPMS U–Pb	36.3 ± 0.3	
		Orebody	Porphyry Cu–Mo orebody	Molybdenite	Re–Os	34.5 ± 0.7 (I)	
O Quy Ho	Lao Cai Province, Vietnam	Orebody	Porphyry Mo orebody	Molybdenite	Re–Os	36.0 ± 1.0 (I)	Tran et al., 2010

I, W and M in parenthesis in the 'age' column represent isochron age, weighted mean model age and model age, respectively.

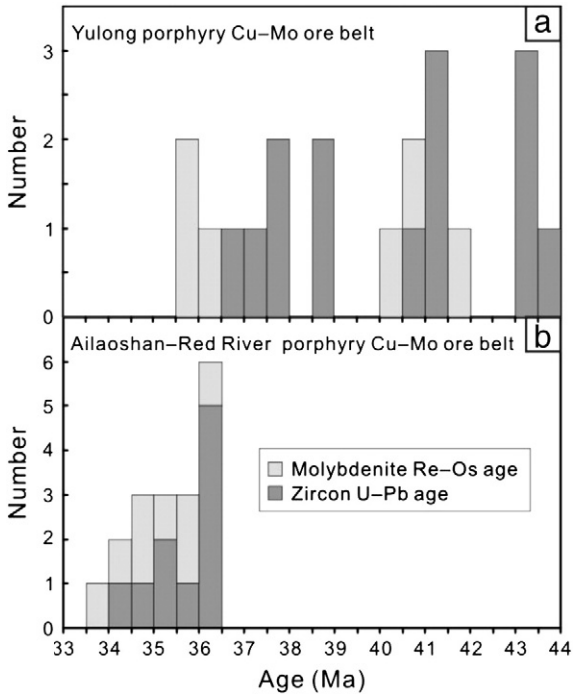

Fig. 6. Histogram of zircon U–Pb and molybdenite Re–Os ages for the Yulong porphyry Cu–Mo ore belt (a), and the Ailaoshan–Red River porphyry Cu–Mo ore belt (b) (age data are from Table 4).

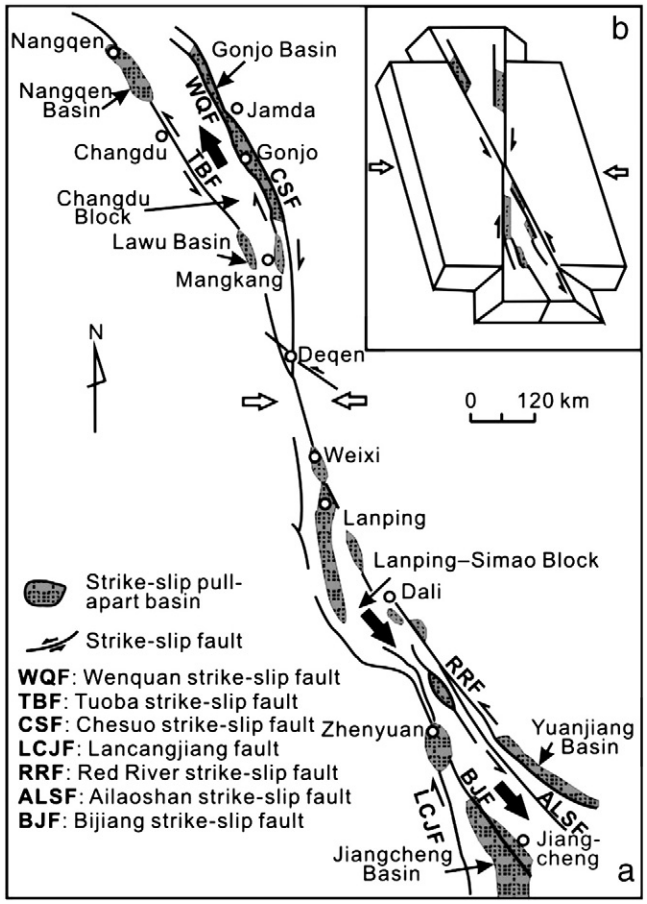

Fig. 7. Proposed strike-slip system and strike-slip pull-apart basin model for eastern Tibet, (a) shows the distribution of the Himalayan strike-slip system and strike-slip pull-apart basin in the Changdu-Simao continental block, (b) a mechanical model for the strike-slip structure (modified from Liu et al., 1993).

precise magmatic emplacement and mineralization ages of porphyry Cu–Mo deposits. New zircon U–Pb and molybdenite Re–Os ages and previous age data of porphyry Cu–Mo deposits in the Jinshajiang–Red River metallogenic belt have been summarized in Table 4 and compiled in Figs. 1 and 6. From these figures, the ages of porphyry Cu–Mo deposits along the Jinshajiang–Red River belt show a remarkable trend. The ages of magmatic emplacement and porphyry Cu–Mo mineralization in the Ailaoshan–Red River ore belt, from north to south, are essentially invariable, and range from 36.3 Ma to 34.6 Ma (ca. 36 Ma), and from 36.0 Ma to 33.9 Ma (ca. 35 Ma), respectively, whereas magmatic emplacement and mineralization ages of porphyry Cu–Mo deposits, from north to south, in the Yulong ore belt vary from 43.8 Ma to 36.9 Ma, and from 41.6 Ma to 35.8 Ma, respectively, with obvious younging towards south. This indicates that various porphyry Cu–Mo deposits in the Jinshajiang–Red River belt formed at different time. The different ages of porphyry Cu–Mo deposits in the Ailaoshan–Red River and Yulong ore belts may reflect distinct geodynamic settings.

5.2. Constraints on the geodynamic environment of the porphyry Cu–Mo mineralization

Although the Jinshajiang and Ailaoshan–Red River strike-slip fault systems are usually regarded as one single system of the Jinshajiang–Red River strike-slip fault, abundant geological evidences, such as strike-slip pull-apart basin, mylonitization and development of lineation and gneissic banding, etc., and relevant geochronological data, indicate that the Jinshajiang and Ailaoshan–Red River strike-slip fault systems underwent divergent tectonic evolutions (Cao et al., 2009; Hou et al., 2003; Liang et al., 2007; Liu et al., 1993; Tapponnier et al., 1990). Under the influence of the Indo-Asian collision, tectonic evolution of the eastern Indo-Asian collision zone was turned into the stage of late-collision transition from ca. 42 Ma, and the corresponding geodynamic setting is a transformation of tectonic stress field from extrusion to extension. This late-collision transition is characterized by relative horizontal movements among various terranes, such as the large-scale strike-slip fault systems, shear systems and thrust systems, distributed in the eastern Indo-Asian collision zone, which absorbed and adjusted the stress and strain produced by the Indo-Asian collision (Fig. 1; Hou et al., 2006, 2007a,c; Wang and Buchifel, 1997; Wang et al., 2001).

Tectonic analyses and relevant geochronological studies indicated that the strike-slip faulting in different sections of the Jinshajiang–Red River strike-slip fault had different patterns in this late-collision transition period. The Jinshajiang strike-slip deep fault system mainly consists of the Chesuo and Wenquan strike-slip faults. Tectonic analysis of strike-slip pull-apart basin of Gonjo, controlled by the Chesuo and Wenquan strike-slip faults, indicated that the Jinshajiang fault system was a right-lateral strike-slip fault system. Furthermore, the fact that the secondary NNW-directed strike-slip faults, such as Riqianma and Laduo faults, derived from the Wenquan strike-slip faulting, have sharp intersection angles with the Wenquan fault, suggested the right-lateral strike-slip motion of the Jinshajiang fault system (Figs. 1 and 3). Various types of alkali-rich volcanics including volcanic breccias and lavas, considered to be triggered by the strike-slip extension, widely developed in the Gonjo, Lawu and Nangqen strike-slip pull-apart basins (Hou et al., 2003; Li et al., 2004; Liu et al., 1993). The dating, mainly using K–Ar and Ar–Ar methods of whole-rock and minerals, of these alkali-rich volcanic rocks in these strike-slip pull-apart basins suggested that the strike-slip motion of the Jinshajiang fault system was initiated from ca. 43 Ma (Hou et al., 2003).

Strike-slip motion along the Ailaoshan–Red River fault system controlled formation of the ASRR shear zone (Fig. 2). Various shear phenomena, such as mylonitization, development of lineation and gneissic banding, controlled by the strike-slip motion, widely developed in the ASRR shear zone. At the same time, various minerals (e.g., muscovite, zircon and monazite, etc.), as the byproducts of these shear phenomena,

were also widely formed. Macro- and micro-structural analyses of these shear phenomena revealed that the Ailaoshan–Red River fault system was a left-lateral strike-slip fault system, though current motion appears to be dextral. Meanwhile, thermochronological dating of these shear phenomena-related minerals, such as muscovite, zircon and monazite, etc., mainly using K–Ar, U–Pb and Th–Pb methods, indicated that the left-lateral strike-slip motion of the Ailaoshan–Red River fault system, was initiated at ca. 36 Ma and lasted until ca. 17 Ma (Figs. 1, 2 and 7; Cao et al., 2009; Chung et al., 1997; Dewey, 1988; Gilley et al., 2003; Harrison et al., 1992, 1996; Leloup et al., 1993, 1995, 2001; Liang et al., 2007; Liu et al., 1993; Schärer et al., 1990, 1994; Tapponnier et al., 1990; Wang et al., 2001; Zhang and Zhong, 1996).

A tectonic model has been established by Liu et al. (1993) and Hou et al. (2003), which can well explain the different strike-slip movements between the Jinshajiang and the Ailaoshan–Red River strike-slip fault systems (Fig. 7). Indo-Asian collision at 70–60 Ma (Yin and Harrison, 2000), resulted in a compressive regime in the eastern Indo-Asian collision zone. Influenced by continued collision between the Indian and Asian continents, from ca. 43 Ma onwards, this collision first caused strike-slip faulting along the Chesuo, Wenquan and Tuoba strike-slip faults in the northern segment of the Jinshajiang–Red River belt (Figs. 3 and 7). Subsequently, from ca. 36 Ma, this collision caused intense E–W compression and conjugate strike-slip movement with an X-shaped structural knot centered just south of the Yulong porphyry Cu–Mo ore belt (Figs. 3 and 7). In this model, the Changdu block was displaced northwestward along several strike-slip faults, such as the Chesuo, Wenquan and Tuoba strike-slip faults, resulting in a group of strike-slip pull-apart basins including the Gonjo, Nangqen and Lawu basins in northern segment of the Jinshajiang–Red River belt. In contrast, the Lanping–Simao block was displaced southeastward along several strike-slip faults, such as the Red River, Ailaoshan and Lancangjiang strike-slip faults, resulting in a group of strike-slip pull-apart basins including the Lanping, Yuanjiang and Jiangcheng basins in southern segment of the Jinshajiang–Red River belt (Fig. 7; Hou et al., 2003). Therefore, it is concluded that there are differences in terms of the strike-slip directions and initial strike-slip ages between the Jinshajiang and Ailaoshan–Red River fault systems.

The difference of the strike-slip movements between the Jinshajiang and Ailaoshan–Red River fault systems can explain different porphyry Cu–Mo mineralization in the Yulong and Ailaoshan–Red River ore belts (Fig. 8). The right-lateral strike-slip motion of the Jinshajiang fault system initiated at ca. 43 Ma with corresponding formation of the Yulong porphyry Cu–Mo system, whereas the left-lateral strike-slip motion of the Ailaoshan–Red River fault system initiated at ca. 36 Ma with corresponding formation of the Ailaoshan–Red River porphyry Cu–Mo system. Therefore, there could be a close relationship between the porphyry Cu–Mo mineralization and relevant strike-slip movements (Fig. 8).

5.3. Role of strike-slip faulting on the formation of porphyry Cu–Mo deposits

The Jinshajiang–Red River porphyry Cu–Mo deposits are primarily distributed along the Jinshajiang–Red River strike-slip fault, which suggests that the regional-scale strike-slip fault system may play a significant role in formation of porphyry Cu–Mo deposits (Hou et al., 2003). Large-scale porphyry emplacement and relevant Cu–Mo mineralization in the Jinshajiang–Red River belt occurred in late or/and post-collisional transpressional and extensional environments at 42–26 Ma (Hou et al., 2007c, 2011). This situation is similar to the 40–30 Ma porphyry Cu–Mo deposits in the Andean magmatic arc (Camus and Dilles, 2001; Richards et al., 2001; Sillitoe, 2010). This can be attributed to the special transpression regime generated by strike-slip faulting, because regional-scale stress regimes, ranging from moderately extensional through oblique slip to contractional, are considered to be favorable for porphyry copper generation (Mungall, 2002; Qin et al., 2005; Richards, 2003; Sillitoe, 2010; Tosdal and Richards, 2001).

Several studies indicate that the alkali-rich igneous rocks in the Jinshajiang–Red River belt, originated from an enriched mantle source (EMII) (Bi et al., 2005; Hou et al., 2003; Jiang et al., 2006; Zhang and Xie, 1997). This enriched mantle source is considered to be a subcontinental lithospheric mantle metasomatized by fluids derived from the ancient Jinshajiang–Ailaoshan subducting oceanic slab (Bi et al., 2005; Hou et al., 2003; Turner et al., 1996). Seismic profiles across the Jinshajiang and Ailaoshan–Red River belts indicate that the Jinshajiang–Red River strike-slip faulting cut through the lithospheric mantle and caused upwelling of hot asthenosphere along the deep fault (Fei, 1983; Liu et al., 2000; Tang and Luo, 1995). This suggests that the Jinshajiang–Red River strike-slip faulting probably caused a depressurization of lithosphere in the region. The depressurization or/and asthenospheric heating could trigger partial melting of the enriched mantle sources of alkali-rich porphyries. Furthermore, the deep strike-slip faults provided the convenient conduits for magmatic migration.

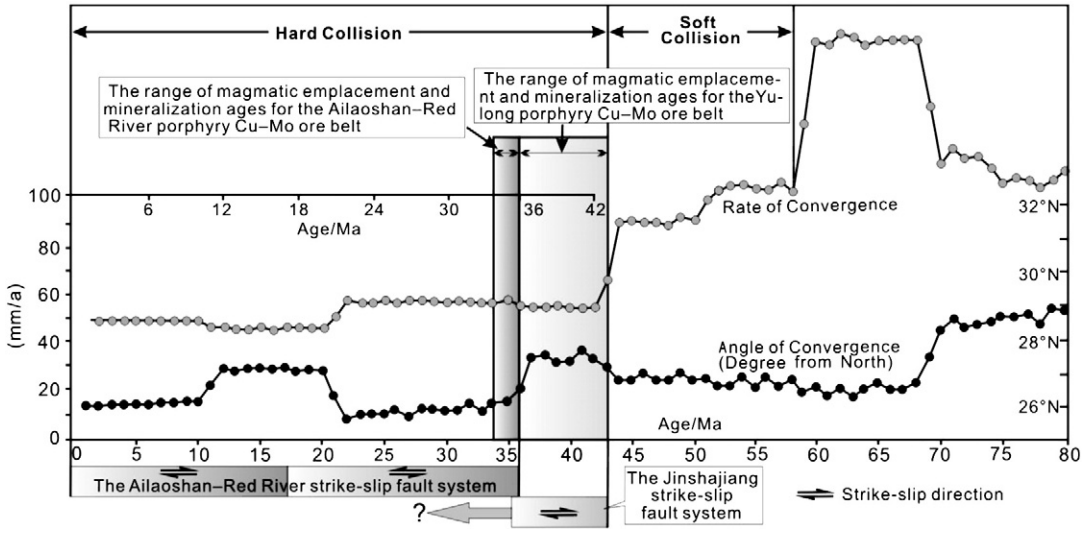

Fig. 8. Rate and angle of convergence between Indian and Asian plates, and relevant strike-slip movement and porphyry Cu–Mo mineralization along the Jinshajiang–Red River metallogenic belt (modified from Lee and Lawver, 1995).

The above factors facilitated formation of alkali-rich porphyries and relevant Cu–Mo deposits along the Jinshajiang–Red River belt (Hou et al., 2003, 2005, 2006; Mo et al., 2006).

6. Conclusions

The porphyry Cu–Mo deposits in the Jinshajiang–Red River metallogenic belt did not form at the same time. The magmatic emplacement and mineralization ages of porphyry Cu–Mo deposits in the Ailaoshan–Red River ore belt range from 36.3 Ma to 34.6 Ma, and from 36.0 Ma to 33.9 Ma, respectively. These ages are obviously younger than the corresponding magmatic emplacement ages of 43.8–36.9 Ma and mineralization ages of 41.6–35.8 Ma of porphyry Cu–Mo deposits in the Yulong ore belt. Reconstruction of the tectonic evolutive history indicates that the geochronological characteristics of the Jinshajiang–Red River porphyry Cu–Mo mineralization are closely related to the divergent strike-slip movements between the Jinshajiang and Ailaoshan–Red River strike-slip faulting resulted from the Indo-Asian collision.

Acknowledgments

This research project is financially supported jointly by “the Key Orientation Project of the Chinese Academy of Sciences (KZCX2-YW-Q04-01), the Natural Science Foundation of China (40873037) and the Key Natural Science Foundation of China (41130423)”. Relevant staffs of Yunnan Honghe Henghao Mining Co. Ltd, Yunnan Copper Industry Co. Ltd and Tibet Yulong Copper Industry Co. Ltd are gratefully acknowledged for their kind help during our fieldwork. We are very grateful to Professor Meifu Zhou (Hong Kong University) and two anonymous referees for their constructive review. Editor-in-Chief Nigel J. Cook is thanked for his editorial comments.

References

Allen, C.R., Gillespie, A.R., Han, Y., Sieh, K.E., Zhang, B., Zhu, C., 1984. Red River and associated faults, Yunnan Province, China: quaternary geology, slip rates, and seismic hazard. Geol. Soc. Am. Bull. 95, 686–700.

Andersen, T., 2002. Correction of common lead in U–Pb analyses that do not report ^{204}Pb. Chem. Geol. 192, 59–79.

Bi, X.W., 1999. Study on alkali-rich intrusive rocks and their relation with metallogenesis of copper and gold in the “Sanjiang” region, western Yunnan. Ph.D. thesis, Institute of Geochemistry, Chinese Academy of Sciences, Guiyang. (in Chinese).

Bi, X.W., Hu, R.Z., Ye, Z.J., Shao, S.X., 1999. Study on the relation between the A-type granite and Cu ore mineralization: evidence from the Machangqing copper deposit. Sci. China D 29, 489–495 (in Chinese).

Bi, X.W., Cornell, D.H., Hu, R.Z., 2002. REE composition of primary and altered feldspar from the mineralized alteration zone of alkali-rich intrusive rocks, western Yunnan province, China. Ore Geol. Rev. 19, 69–78.

Bi, X.W., Hu, R.Z., Cornell, D.H., 2004. Trace element and isotope evidence for the evolution of ore-forming fluid of Yao'an gold deposit, Yunnan province, China. Miner. Deposita 39, 21–30.

Bi, X.W., Hu, R.Z., Peng, J.T., Wu, K.X., Su, W.C., Zhan, X.Z., 2005. Geochemical characteristics of the Yao'an and Machangqing alkaline-rich intrusions. Acta Petrol. Sin. 21, 113–124 (in Chinese with English abstract).

Bi, X.W., Hu, R.Z., Mungall, J.E., Hanley, J.J., Peng, J.T., Wu, K.X., Li, H.L., 2006. Mineral chemistry studies of Cu- and Au-mineralized alkaline intrusions. Acta Mineral. Sin. 26, 377–386 (in Chinese with English abstract).

Bi, X.W., Hu, R.Z., Hanley, J.J., Mungall, J., Peng, J.T., Shang, L.B., Wu, K.X., Suang, Y., Li, H.L., Hu, X.Y., 2009. Crystallisation conditions (T, P, fO_2) from mineral chemistry of Cu- and Au-mineralised alkaline intrusions in the Red River–Jinshajiang alkaline igneous belt, western Yunnan Province, China. Mineral. Petrol. 96, 43–58.

Camus, F., Dilles, J.H., 2001. A special issue devoted to porphyry copper deposits of northern Chile: preface. Econ. Geol. 96, 233–237.

Cao, S.Y., Liu, J.L., Bernd, L.E., Axel, V., Zou, Y., Zhao, C.Q., 2009. Timing of initiation of left-lateral slip along the Ailaoshan–Red River shear zone: microstructural, texture and thermochronological evidence from high temperature mylonites in Diancang Shan, SW China. Acta Geol. Sin. 10, 1388–1400 (in Chinese with English abstract).

Chung, S.L., Lee, T.Y., Lo, C.H., Wang, P.L., Chen, C.Y., Yem, N.T., Hoa, T.T., Wu, G.Y., 1997. Intraplate extension prior to continental extrusion along the Ailao Shan–Red River shear zone. Geology 25, 311–314.

Chung, S.L., Lo, C.H., Lee, T.Y., Zhang, Y.Q., Xie, Y.W., Li, X.H., Wang, K.L., Wang, P.L., 1998. Diachronous uplift of the Tibetan plateau starting 40 Myr ago. Nature 394, 769–773.

Deng, W.M., Huang, X., Zhong, D.L., 1998. Alkali-rich porphyry and its relation with intraplate deformation of north part of Jinsha River belt in western Yunnan, China. Sci. China D 28, 111–117 (in Chinese).

Dewey, J.F., 1988. Extensional collapse of orogens. Tectonics 7, 1123–1139.

Du, A.D., He, H.L., Yin, N.W., Zhou, X.Q., Sun, Y.L., Sun, D.Z., Chen, S.Z., Qu, W.J., 1994. The study on the analytical methods of Re–Os age for molybdenites. Acta Geol. Sin. 68, 339–347 (in Chinese with English abstract).

Du, A.D., Zhao, D.M., Wang, S.X., Sun, D.Z., Liu, D.Y., 2001. Precise Re–Os dating for Molybdenite by ID-NTIMS with Carius tube sample preparation. Rock Miner. Anal. 20, 247–252 (in Chinese with English abstract).

Du, A.D., Wu, S.Q., Sun, D.Z., Wang, S.X., Qu, W.J., Markey, R., Stain, H., Morgan, J., Malinovskiy, D., 2004. Preparation and certification of Re–Os dating reference materials: molybdenites HLP and JDC. Geostand. Geoanal. Res. 28, 41–52.

Fei, D., 1983. Regional structure in the northern part of the South China Sea and transition from continental crust to oceanic crust. J. Geophys. 26, 459–467 (in Chinese with English abstract).

Gilley, L.D., Harrison, T.M., Leloup, P.H., Ryerson, F.J., Lovera, O.M., Wang, J.H., 2003. Direct dating of left–lateral deformation along the Red River shear zone, China and Vienam. J. Geophys. Res. http://dx.doi.org/10.1029/2001JB001726.

Gu, X.X., Tang, J.X., Wang, C.S., Chen, J.P., He, B.B., 2003. Himalayan magmatism and porphyry copper–molybdenum mineralization in the Yulong ore belt, East Tibet. Mineral. Petrol. 78, 1–20.

Guo, L.G., Liu, Y.P., Xu, W., Zhang, X.C., Qin, K.Z., Li, T.S., Shi, Y.R., 2006. Constraints to the mineralization age of the Yulong porphyry copper deposit from SHRIMP U–Pb zircon data in Tibet. Acta Petrol. Sin. 21, 1009–1016 (in Chinese with English abstract).

Harrison, T.M., Chen, W., Leloup, P.H., Ryerson, F.J., Tapponnier, P., 1992. An early Miocene transition in deformation regime within the Red River fault zone, Yunnan, and its significance for the Indo-Asian tectonics. J. Geophys. Res. 97, 7159–7182.

Harrison, T.M., Leloup, P.H., Ryerson, F.J., Tapponnier, P., Lacassin, R., Chen, W.J., 1996. Diachronous initiation of transtension along the Ailao Shan–Red River shear zone, Yunnan and Vietnam. In: Yin, A., Harrison, T.M. (Eds.), The Tectonic Evolution of Asia. Cambridge University Press, New York, pp. 208–226.

He, W.Y., Mo, X.X., Yu, X.H., Li, Y., Huang, X.K., He, Z.H., 2011. Geochronological study of magmatic intrusions and mineralization of Machangqing porphyry Cu–Mo–Au deposit, western Yunnan Province. Earth Sci. Front. 1, 207–215 (in Chinese with English abstract).

Hou, Z.Q., Ma, H.W., Zaw, K., Zhang, Y.Q., Wang, M.J., Wang, Z., Pan, G.T., Tang, R.L., 2003. The Himalayan Yulong porphyry copper belt: product of large-scale strike-slip faulting in eastern Tibet. Econ. Geol. 98, 125–145.

Hou, Z.Q., Lu, Q.T., Qu, X.M., Nie, F.J., Meng, X.J., Li, Z.Q., Yang, Z.S., Mo, X.X., Wang, A.J., Li, X.B., Wang, Z.Q., Wang, E.C., 2005. Metallogenesis in the Tibetan collisional orogenic belt. Mineral Deposit Research: Meeting the Global Challenge. Springer, pp. 1231–1233.

Hou, Z.Q., Zeng, P.S., Gao, Y.F., Du, A.D., Fu, D.M., 2006. Himalayan Cu–Mo–Au mineralization in the eastern Indo-Asian collision zone: constraints from Re–Os dating of molybdenite. Miner. Deposita 41, 33–45.

Hou, Z.Q., Zaw, K., Pan, G.T., Mo, X.X., Xu, Q., Hu, Y.Z., Li, X.Z., 2007a. Sanjiang Tethyan metallogenesis in SW China: tectonic setting, metallogenic epochs and deposit types. Ore Geol. Rev. 31, 48–87.

Hou, Z.Q., Xie, Y.L., Xu, W.Y., Li, Y.Q., Zhu, X.K., Khin, Z., Beaudoin, G., Rui, Z.Y., Wei, H.A., Ciren, L., 2007b. Yulong deposit, eastern Tibet: a high-sulfidation Cu–Au porphyry copper deposit in the eastern Indo-Asian collision zone. Int. Geol. Rev. 49, 235–258.

Hou, Z.Q., Pan, X.F., Yang, Z.M., Qu, X.M., 2007c. Porphyry Cu–(Mo–Au) deposits no related to oceanic-slab subduction: examples from Chinese porphyry deposits in continental setting. Geoscience 21, 332–351 (in Chinese with English abstract).

Hou, Z.Q., Zhang, H.R., Pan, X.F., Yang, Z.M., 2011. Porphyry Cu (–Mo–Au) deposits related to melting of thickened mafic lower crust: examples from the eastern Tethyan metallogenic domain. Ore Geol. Rev. 39, 21–45.

Hu, R.Z., Burnard, P.G., Turner, G., Bi, X.W., 1998. Helium and argon systematics in fluid inclusions of Machangqing copper deposit in west Yunnan province, China. Chem. Geol. 146, 55–63.

Hu, R.Z., Burnard, P.G., Bi, X.W., Zhou, M.F., Pen, J.T., Su, W.C., Wu, K.X., 2004. Helium and argon isotope geochemistry of alkaline intrusion-associated gold and copper deposits along the Red River–Jingshajiang fault belt, SW China. Chem. Geol. 203, 305–317.

Huang, B., Liang, H.Y., Mo, J.H., Xie, Y.W., 2009. Zircon LA-ICP-MS U–Pb age of the Jinping–Tongchang porphyry associated with Cu–Mo mineralization and its geological implication. Geotecton. Metallog. 33, 598–602 (in Chinese with English abstract).

Jiang, Y.H., Jiang, S.Y., Ling, H.F., Dai, B.Z., 2006. Low-degree melting of a metasomatized lithospheric mantle for the origin of Cenozoic Yulong monzogranite-porphyry, east Tibet: Geochemical and Sr–Nd–Pb–Hf isotopic constraints. Earth Planet. Sci. Lett. 241, 617–633.

Lacassin, R., Scharer, U., Leloup, P.H., Arnaud, N., Tapponnier, P., Liu, X.H., Zhang, L.S., 1996. Tertiary deformation and metamorphism SE of Tibet: the folded tiger-leap decollement of NW Yunnan, China. Tectonics 15, 605–622.

Lee, T.Y., Lawver, L.A., 1995. Cenozoic plate reconstruction of Southeast Asia. Tectonophysics 251, 85–138.

Leloup, P.H., Harrison, T.M., Ryerson, F.J., Chen, W.J., Li, Q., Tapponnier, P., Lacassin, R., 1993. Structural, petrological and thermal evolution of a Tertiary ductile strike-slip shear zone, Diancang Shan, Yunnan. J. Geophys. Res. 98, 6715–6743.

Leloup, P.H., Lacassin, R., Tapponnier, P., Scharer, U., Zhong, D.L., Liu, X.H., Zhang, L.S., Ji, S.C., Trinh, P.T., 1995. The Ailao Shan–Red River shear zone (Yunnan, China), Tertiary transform boundary of Indo–china. Tectonophysics 251, 3–84.

Leloup, P.H., Arnaud, N., Lacassin, R., Kienast, J.R., Harrison, T.M., Trong, T.T.P., Replumaz, A., Tapponnier, P., 2001. New constraints on the structure, thermochronology, and timing of the Ailao Shan–Red River shear zone, SE Asia. J. Geophys. Res. 106, 6683–6732.

Li, Z.X., Chen, Z.L., Li, X.Z., Gizbert, C., Burchfiel, B.C., 2004. K–Ar ages of Cenozoic volcanic rocks from Gongjue basin in eastern Tibet. Earth Sci. J. China Univ. Geosci. 29, 278–282 (in Chinese with English abstract).

Liang, H.Y., 2002. New advances in study of porphyry copper diagenetic metallogenetic process in the southeastern margin of Qinghai Xizang (Tibet) plateau. Miner. Deposits 7, 365 (in Chinese).

Liang, H.Y., Campbell, I.H., Xie, Y.W., Zhang, Y.Q., 2002. Zircon age dated by ELA-ICP-MS for ore-bearing porphyry in Jinping Tongchang. Miner. Deposits 7, 421–422 (in Chinese).

Liang, H.Y., Xie, Y.W., Zhang, Y.Q., Campbell, I.H., 2004. Constraints to the mineralization of the copper deposits from forming and evolution of potassium-rich alkali rock at Machangqing copper deposits. Prog. Nat. Sci. 14, 116–119 (in Chinese with English abstract).

Liang, H.Y., Campbell, I.H., Allen, C., Sun, W.D., Liu, C.Q., Yu, H.X., Xie, Y.W., Zhang, Y.Q., 2006a. Zircon Ce^{4+}/Ce^{3+} ratios and ages for Yulong ore-bearing porphyries in eastern Tibet. Miner. Deposita 41, 152–159.

Liang, H.Y., Yu, H.X., Mo, C.H., Zhang, Y.Q., Xie, Y.W., 2006b. Zircon LA-ICP-MS U–Pb age, Ce^{4+}/Ce^{3+} ratios and the geochemical features of the Machangqing complex associated with copper deposit. Chin. J. Geochem. 25, 223–229.

Liang, H.Y., Campbell, I.H., Allen, C.M., Sun, W.D., Yu, H.X., Xie, Y.W., Zhang, Y.Q., 2007. The age of the potassic alkaline igneous rocks along the Ailao Shan–Red River shear zone: implications for the onset age of left-lateral shearing. J. Geol. 115, 231–242.

Liang, H.Y., Mo, J.H., Sun, W.D., Yu, H.X., Zhang, Y.Q., Allen, C.M., 2008. Study on the duration of the ore-forming system of the Yulong giant porphyry copper deposit in eastern Tibet, China. Acta Petrol. Sin. 24, 2352–2358 (in Chinese with English abstract).

Liang, H.Y., Sun, W.D., Su, W.C., Zartman, R.E., 2009a. Porphyry copper–gold mineralization at Yulong, China, promoted by decreasing redox potential during magnetite alteration. Econ. Geol. 104, 587–596.

Liang, H.Y., Mo, J.H., Sun, W.D., Zhang, Y.Q., Zeng, T., Hu, G.Q., Allen, C.M., 2009b. Study on geochemical composition and isotope ages of the Malasongduo porphyry associated with Cu–Mo mineralization. Acta Petrol. Sin. 25, 385–392 (in Chinese with English abstract).

Liu, Z.Q., Li, X.Z., Ye, Q.T., Luo, J.N., Shen, G.F., 1993. Division of tectonomagmatic belts and the distribution of deposits in the Sanjiang area. Geological Publishing House, Beijing. 246 pp. (in Chinese with English abstract).

Liu, F.T., Liu, J.H., He, J.K., You, Q.Y., 2000. The subduction slab of Yangtze block under Tethysian oregen in western Yunnan Province. Chin. Sci. Bull. 45, 79–84 (in Chinese).

Liu, Y.S., Hu, Z.C., Gao, S., Günther, D., Xu, J., Gao, C.G., Chen, H.H., 2008. In situ analysis of major and trace elements of anhydrous minerals by LA-ICP-MS without applying an internal standard. Chem. Geol. 257, 34–43.

Liu, Y.S., Gao, S., Hu, Z.C., Gao, C.G., Zong, K.Q., Wang, D.B., 2010a. Continental and oceanic crust recycling-induced melt-peridotite interactions in the trans-north China orogen: U–Pb dating, Hf isotopes and trace elements in zircons from mantle xenoliths. J. Petrol. 51, 537–571.

Liu, Y.S., Hu, Z.C., Zong, K.Q., Gao, C.G., Gao, S., Xu, J.A., Chen, H.H., 2010b. Reappraisement and refinement of zircon U–Pb isotope and trace element analyses by LA-ICP-MS. Chin. Sci. Bull. 55, 1535–1546.

Ludwig, K.R., 2001. Users manual for isoplot/ex (rev. 2.49): a geochronological toolkit for Microsoft Excel. Berkeley Geochronology Center Special Publication, 1, pp. 1–55.

Mo, X.X., Zhao, Z.D., Deng, J.F., Flower, M., Yu, X.H., Luo, Z.H., Li, Y.G., Zhou, S., Dong, G.C., Zhu, D.C., Wang, L.L., 2006. Petrology and geochemistry of postcollisional volcanic rocks from the Tibetan plateau: implications for lithosphere heterpgeneity and collision-induced asthenpsheric mantle flow. Geol. Soc. Am. Spec. Pap. 409, 507–530.

Mungall, J.E., 2002. Roasting the mantle: slab melting and the genesis of major Au and Au-rich Cu deposits. Geology 30, 915–918.

Peltzer, G., Tapponnier, P., 1988. Formation of strikeslip faults, rifts, and basins during the India–Asia collision: an experimental approach. J. Geophys. Res. 93, 15085–15117.

Qin, K.Z., Tosdal, R.M., Li, G.M., Zhang, Q., Li, J.L., 2005. Formation of the Miocene porphyry Cu (–Mo–Au) deposits in the Gangdese arc, southern Tibet, in a transitional tectonic setting. Mineral Deposit Research: Meeting the Challenge, vol. 3. China Land Publishing House, Beijing, pp. 44–47.

Qu, W.J., Du, A.D., 2003. Highly precise Re–Os dating of molybdenite by ICP-MS with carius tube sample digestion. Rock Miner. Anal. 22, 254–257 (in Chinese with English abstract).

Replumaz, A., Lacassin, R., Tapponnier, P., Leloup, P.H., 2001. Large river offsets and Plio-Quaternary dextral slip rate on the Red River fault (Yunnan, China). J. Geophys. Res. 106, 819–836.

Richards, J.P., 2003. Tectono-magmatic precursors for porphyry Cu–(Mo–Au) deposit formation. Econ. Geol. 98, 1515–1533.

Richards, J.P., Boyce, A.J., Pringle, M.S., 2001. Geologic evolution of the Escondida area, northern Chile: a model for spatial and temporal localization of porphyry Cu mineralization. Econ. Geol. 96, 271–305.

Sato, K., Liu, Y.Y., Zhu, Z.C., Yang, Z.Y., Otofuji, Y., 1999. Paleomagnetic study of middle Cretaceous rocks from Yunlong, western Yunnan, China: evidence of southward displacement of Indochina. Earth Planet. Sci. Lett. 165, 1–15.

Schärer, U., Tapponnier, P., Lacassin, R., Leloup, P.H., Zhong, D.L., Ji, S.C., 1990. Intraplate tectonics in Asia: a precise age for large-scale Miocene movement along the Ailao Shan–Red River shear zone, China. Earth Planet. Sci. Lett. 97, 65–77.

Schärer, U., Zhang, L.C., Tapponnier, P., 1994. Duration of strike-slip movements in large shear zones: the Red River belt, China. Earth Planet. Sci. Lett. 126, 379–397.

Selby, D., Creaser, R.A., 2001. Re–Os geochronology and systematics in molybdenite from the Endako porphyry molybdenum deposit, British Columbia, Canada. Econ. Geol. 96, 197–204.

Sillitoe, R.H., 2010. Porphyry copper systems. Econ. Geol. 105, 3–41.

Smoliar, M.I., Walker, R.J., Morgan, J.W., 1996. Re–Os ages of group IIA, IIIA, IVA and IVB iron meteorites. Science 271, 1099–1102.

Stein, H.J., Markey, R.J., Morgan, J.W., Du, A., Sun, Y., 1997. Highly precise and accurate Re–Os ages for molybdenite from the east Qinling molybdenum belt, Shanxi Province, China. Econ. Geol. 92, 827–835.

Tang, R.L., Luo, H., 1995. The geology of Yulong porphyry copper (molybdenum) ore belt, Xizang (Tibet). Geological Publishing House, Beijing. 320 pp. (in Chinese with English abstract).

Tang, J.X., Wang, C.H., Qu, W.J., Du, A.D., Ying, L.J., Gao, Y.M., 2009. Re–Os isotopic dating of molybdenite from the Yulong porphyry copper–molybdenum deposit in Tibet and its Metallogenic significance. Rock Miner. Anal. 28, 215–218 (in Chinese with English abstract).

Tapponnier, P., Molnar, P., 1977. Active faulting and tectonics in China. J. Geophys. Res. 82, 2905–2930.

Tapponnier, P., Peltzer, G., Ledain, A.Y., Armijo, R., Cobbold, P., 1982. Propagating extension tectonics in Asia: new insights from simple experiments with plasticine. Geology 10, 611–616.

Tapponnier, P., Peltzer, G., Armijo, R., 1986. On the mechanics of the collision between Indian and Asia. In: Coward, M.P., Ries, A.C. (Eds.), Collision Tectonics: Geological Society of London Special Publication, 19, pp. 1154–1157.

Tapponnier, P., Lacassin, R., Leloup, P.H., Schärer, U., Zhong, D.L., Wu, H.W., Liu, X.H., Ji, S.C., Zhang, L.S., Zhong, J.Y., 1990. The Ailao Shan/Red River metamorphic belt: Tertiary left-lateral shear between Indochina and South China. Nature 343, 431–437.

Tosdal, R.M., Richards, J.P., 2001. Magmatic and structural controls on the development of porphyry Cu ± Mo ± Au deposits. Rev. Econ. Geol. 14, 157–181.

Tran, M.D., Liu, J.L., Nguyen, Q.L., Chen, Y., Zou, Y.X., 2010. Metallogenic epoch and metall ic sources of O Quy Ho molybdenum deposit, Vietnam. Miner. Deposits 29, 371–378 (in Chinese with English abstract).

Turner, S., Arnaud, N., Liu, J., Rogers, N., Hawkesworth, C., Harris, N., Kelley, S., Vancalsteren, P., Deng, W., 1996. Post-collision, shoshonitic volcanism on the Tibetan plateau: implications for convective thinning of the lithosphere and the source of ocean island basalts. J. Petrol. 37, 45–71.

Wang, E.C., Buchifel, B.C., 1997. Interpretation of Cenozoic tectonics in the right-lateral accommodation zone between the AilaoShan shear zone and the eastern Himalayan syntaxis. Int. Geol. Rev. 39, 191–219.

Wang, J.H., Yin, A., Harrison, T.M., Grove, M., Zhang, Y.Q., Xie, G.H., 2001. A tectonic model for Cenozoic igneous activities in the eastern Indo-Asian collision zone. Earth Planet. Sci. Lett. 88, 123–133.

Wang, D.H., Qu, W.J., Li, Z.W., Ying, H.L., Chen, Y.C., 2004. The metallogenic concentrating epoch of the Porphyry Copper (molybdenum) deposits in Jinshajiang–Red River metallogenic belt: Re–Os isotope dating. Sci. China D 34, 345–349 (in Chinese).

Wang, Z.L., Yang, Z.M., Yang, Z.S., Tian, S.H., Liu, Y.C., Ma, Y.Q., Wang, G.R., Qu, W.J., 2008. Narigongma porphyry molybdenite copper deposit, northern extension of Yulong copper belt: evidence from the age of Re–Os isotope. Acta Petrol. Sin. 24, 503–510 (in Chinese with English abstract).

Wang, C.H., Tang, J.X., Chen, J.P., Hao, J.H., Gao, Y.M., Liu, Y.W., Fan, T., Zhang, Q.Z., Ying, L.J., Chen, Z.J., 2009. Chronological research of Yulong copper–molybdenum porphyry deposit. Acta Geol. Sin. 83, 1445–1455 (in Chinese with English abstract).

Wu, R., Liu, X.F., Xiao, J.X., Fan, P., 2010. Geochronology of intrusive and ore at Machangqing deposit. Miner. Deposits 29, 521–522 (in Chinese).

Xie, Y.W., Zhang, Y.Q., Hu, G.X., 1984. A preliminary study on geochemical characteristics and mineralization specificity of alkaline-rich intrusive belt in Ailaoshan–Jinshajiang. J. Kunming Univ. Sci. Technol. (4), 1–16 (in Chinese with English abstract).

Xing, J.B., Guo, X.D., Qu, W.J., Wang, Z.H., Li, H.G., 2009. Molybdenite Re–Os age and other geological meaning of Machangqing porphyry copper, molybdenum deposit. Gold Sci. Technol. 17, 24–29 (in Chinese with English abstract).

Xu, L.L., 2011. The diagenetic and metallogenic geochronology and magmatic *f*O2 characteristics of Jinshajiang-Red River porphyry Cu (Mo Au) metallogenic systems. Ph.D. thesis, Institute of Geochemistry, Chinese Academy of Sciences, Guiyang. (in Chinese with English abstract).

Xu, X.W., Cai, X.P., Xiao, Q.B., Peters, S.G., 2007. Porphyry Cu–Au and associated polymetallic Fe–Cu–Au deposits in the Beiya Area, western Yunnan Province, south China. Ore Geol. Rev. 31, 224–246.

Xu, L.L., Bi, X.W., Su, W.C., Qi, Y.Q., Li, L., Chen, Y.W., Dong, S.H., Tang, Y.Y., 2011. Geochemical characteristics and petrogenesis of the quartz syenite porphyry from Tongchang porphyry Cu (Mo–Au) deposit in Jinping County, Yunan Province. Acta Petrol. Sin. 27, 3109–3122 (in Chinese with English abstract).

Xue, B.G., 2008. On the division of Au metallogenetic zone and metallogenetic rule in Yunnan. Yunan Geol. 27, 261–277 (in Chinese with English abstract).

Yang, Z.Y., Besse, J., Sutheetorn, V., Bassoullet, J.P., Fontaine, H., Buffetaut, E., 1995. Lower–Middle Jurassic paleomagnetic data from the Mae Sot area (Thailand): paleogeographic evolution and deformation history of southeastern Asia. Earth Planet. Sci. Lett. 136, 325–341.

Yang, Z.M., Hou, Z.Q., Yang, Z.S., Wang, S.X., Wang, G.R., Tian, S.H., Wen, D.Y., Wang, Z.L., Liu, Y.C., 2008. Genesis of porphyries and tectonic controls to the Narigongma porphyry Mo (–Cu) deposit, southern Qinghai. Acta Petrol. Sin. 24, 489–502 (in Chinese with English abstract).

Yin, A., Harrison, T.M., 2000. Geologic evolution of the Himalayan–Tibetan orogen. Annu. Rev. Earth Planet. Sci. 28, 211–280.

York, D., 1969. Least squares fitting of a straight line with correlated errors. Earth Planet. Sci. Lett. 5, 320–324.

Zeng, P.S., Mo, X.X., Yu, X.H., 2002. Nd, Sr and Pb isotopic characteristics of the alkaline-rich porphyries in western Yunnan and its compression strike-slip setting. Acta Petrol. Mineral. 21, 231–241 (in Chinese with English abstract).

Zhang, L.S., Schärer, U., 1999. Age and origin of magmatism along the Cenozoic Red River shear belt, China. Contrib. Mineral. Petrol. 134, 67–85.
Zhang, Y.Q., Xie, Y.W., 1997. Nd, Sr isotopic character and chronology of Ailaoshan–Jinshajiang alkali-rich intrusive rocks. Sci. China 27, 289–293 (in Chinese).
Zhang, L.S., Zhong, D.L., 1996. The Red River strike-slip shear zone and Cenozoic tectonics of east Asia continent. Sci. Geol. Sin. 31, 327–340 (in Chinese with English abstract).
Zhang, Y.Q., Xie, Y.W., Tu, G.C., 1987. A preliminary study on the relationship between rift and Ailaoshan–Jianshajiang alkaline intrusive rocks. Acta Petrol. Sin. 1, 17–26 (in Chinese with English abstract).
Zhu, X.P., 2010. Geological characteristics and metallogenesis in Habo porphyry Cu–Mo–Au deposit, Yunan, China. Ph.D. thesis, China University of Geosciences, Beijing. (in Chinese with English abstract).